CONFIDENTIAL

Copy 172
RM L54L07

CLASSIFICATION CHANGED TO: Unclassified
Per Abstract 121, 11-4-57

NACA RM L54L07

CASE FILE COPY

NACA

MAR 15 1955

RESEARCH MEMORANDUM

FLIGHT MEASUREMENTS OF THE TRANSONIC DRAG OF MODELS OF SEVERAL ISOLATED EXTERNAL STORES AND NACELLES

By Joseph E. Stevens and Paul E. Purser

Langley Aeronautical Laboratory
Langley Field, Va.

CLASSIFIED DOCUMENT

This material contains information affecting the National Defense of the United States within the meaning of the espionage laws, Title 18, U.S.C., Secs. 793 and 794, the transmission or revelation of which in any manner to an unauthorized person is prohibited by law.

NATIONAL ADVISORY COMMITTEE
FOR AERONAUTICS

WASHINGTON
March 11, 1955

CONFIDENTIAL

NATIONAL ADVISORY COMMITTEE FOR AERONAUTICS

RESEARCH MEMORANDUM

FLIGHT MEASUREMENTS OF THE TRANSONIC DRAG OF MODELS OF SEVERAL ISOLATED EXTERNAL STORES AND NACELLES

By Joseph E. Stevens and Paul E. Purser

SUMMARY

Drag measurements have been made on models of 20 isolated external stores and nacelles which were flown from the helium gun at Wallops Island, Va., at Mach numbers between 0.8 and 1.3 and Reynolds numbers between 3×10^6 and 12×10^6, based on body length.

The data agreed fairly well in drag-rise Mach number and peak-pressure drag with the correlation of body-drag data presented in NACA RM L53I22c.

INTRODUCTION

The National Advisory Committee for Aeronautics, for several years, has been investigating the drag of various combinations of wings, bodies, and external stores or nacelles. (See refs. 1 to 10, for example.) In the majority of these studies no measurements of the drag of the isolated store have been available for use in separating the interference component from the store-plus-interference drag. The present tests were undertaken to provide these isolated-store drag data.

The models used duplicated the store and nacelle shapes of references 3 to 14 and included some other store and nacelle shapes for which the complete investigations are unpublished. All the models were flown from the helium gun at Wallops Island, Va., described briefly in reference 1, at Mach numbers between 0.8 and 1.3 and Reynolds numbers between 3×10^6 and 12×10^6.

Although the general concept of interference drag has been modified to some extent by the investigations reported in references 15 and 16, a knowledge of the drags of the isolated components of various wing-body combinations is useful. This report presents the drag data for the

various store and nacelle shapes, along with a brief comparison of these data with the body-drag correlation of reference 17.

SYMBOLS

C_D drag coefficient, $\frac{D}{qS}$

ΔC_D peak-pressure drag coefficient, Maximum supersonic C_D - Subsonic C_D

S area, sq ft

D drag, lb

q dynamic pressure, $\frac{\rho}{2} V^2$, lb/sq ft

V velocity, ft/sec

ρ mass density of air, slug/cu ft

M Mach number

M_{DR} drag-rise Mach number, where $\frac{dC_D}{dM} = 1.0$

R Reynolds number, $\frac{\rho V l}{\mu}$

μ viscosity of air, slugs/ft-sec

l body length, ft

l' body length, neglecting cylindrical portion, ft

d body maximum diameter, ft

d_b body base diameter, ft

c streamwise fin chord, ft

f drag-rise correlation factor, $\int_0^1 \left[\frac{d\left(r/r_{max}\right)^2}{d(x/l')}\right]^2 d(x/l')$

r	body radius at any station, ft
r_{max}	body maximum radius, ft
x	longitudinal station on body, measured from nose, ft
$(l/d)_e$	extremity (nose or afterbody) fineness ratio

MODELS AND TESTS

Models

Ordinates of all the models tested are given in table I, and a photograph of one of the models is shown in figure 1. All the models had maximum diameters of 1.50 inches, weighed approximately $1\frac{1}{4}$ pounds, and were constructed of various combinations of wood and metal. All the models were stabilized by three fins having hexagonal airfoil sections 0.0278c thick streamwise, 45° of sweepback, and no taper. (See fig. 2.) For all models the fin chord was 1.80 inches and the exposed span, measured from the intersection of the 0.50c line with the body side, was 1.74 inches per fin.

The models were accelerated to maximum velocity (M between 1.3 and 1.4) by the helium gun shown in figure 3. The sabot, push plate, and push cup (shown in fig. 1) separated from the models shortly after leaving the muzzle of the gun. The pointed-base models were adapted to the push cup by filling the cup with a plastic material to prevent metal-to-metal contact and model distortion. The afterbodies of two of the models were so slender that, in addition to the plastic adapter, a step was machined on the body to take the thrust of the push cup.

Tests

As noted previously, the models were accelerated to maximum velocity by the helium gun (fig. 3). After the models were in free flight, the velocity was recorded by the CW Doppler radar set shown near the gun muzzle in figure 3. Radiosondes, released near the time of firing, provided data on atmospheric pressure, temperature, and winds over the firing range. Model flight paths were calculated as ballistic trajectories; spot checks, in which such calculated flight paths were compared to those measured with a modified SCR 584 radar set, showed that the calculations were acceptable for the dense, symmetrical, zero-lift models flown at low elevation angles.

The velocity-time data were differentiated to provide longitudinal accelerations. Drag coefficients were obtained from the acceleration and atmospheric data in conjunction with the calculated flight path. Analyses and comparisons of data from duplicate helium-gun models indicate that in general the accuracy of the data is within the following limits:

	Supersonic	Subsonic
C_D (based on frontal area)	±0.005	±0.01
M	±0.005	±0.01

DATA

Fins

Drag data for the standard fins with which all the models were equipped are shown in figure 4. The fins were mounted on a slender cone-cylinder body (fig. 4(a)) and the drag of the complete configuration was measured. Figure 4(b) shows a partial breakdown of the drag based on the store frontal area of 0.0123 sq ft. The drag of the cone-cylinder body was established by using experimental base drag previously measured, cone drag from standard cone tables, and skin-friction drag calculated by assuming a turbulent boundary layer.

Bodies

Figures 5(a) to 5(t) present, for each body tested, the variation of Reynolds number, total drag, and total drag minus fin drag (where the fin drag was obtained from fig. 4) with Mach number. The total drag minus fin drag is designated "total-fin" in figure 5. An index to the figures which present the basic drag data for each body is given in table II.

As noted previously, two of the models had thrust steps machined on the afterbody; these models were the NACA 65A-series body with $l/d = 10.00$ and NACA 65-series body with $l/d = 10.68$, figures 5(c) and 5(d), respectively. Estimates, based on references 18 and 19, indicate that the steps may have caused an increase in C_D of about 0.009 at supersonic speeds and 0.004 at subsonic speeds for these two models. These values amount to about 4 percent of the total drag minus fin drag.

RESULTS AND DISCUSSION

Among the various bodies tested there were several families where systematic changes were made in shape or fineness ratio. The data for these families are presented as total C_D minus fin C_D in the comparison plots of figures 6 and 7.

The data for all bodies tested are presented in figures 8 to 10 in terms of body-drag correlation parameters of reference 17.

Fineness-Ratio and Shape Effects

NACA 65A series.- Data for the NACA 65A-series bodies of various fineness ratios and that for the F-84 tank which has a similar profile are compared in figure 6(a). The data show the expected increase in M_{DR} and decrease in supersonic C_D with increases in fineness ratio. The drag coefficient C_D for the F-84 tank ($l/d = 7.43$) falls very close to C_D for the NACA 65A-series body ($l/d = 8.00$); the differences below $M = 1.1$ are in the expected direction, and the tendency toward lower peak supersonic drag for the F-84 tank is probably a reflection of the higher fineness-ratio nose on this body. The NACA 65A-series bodies show a slight decrease in subsonic drag level with increasing fineness ratio whereas, generally, the other bodies tested show increasing subsonic drag level with increasing fineness ratio. The variation shown by the NACA 65A-series is, however, within the experimental accuracy of the data.

Circular-arc series.- Data for the circular-arc body series are compared in figure 6(b). The circular-arc-series data show the expected effects of fineness ratio on M_{DR} and peak-pressure drag with subsonic differences that are within the experimental accuracy as was also shown by the data on the NACA 65A-series bodies.

DAC store series.- Data for the standard DAC store shape and an elongated DAC shape are compared in figure 6(c). Elongating the DAC store gave the expected increase in M_{DR} and decrease in pressure drag, but the accompanying increase in friction drag resulted in higher total drag for the elongated store at $M < 1.03$. In an actual installation, the difference in interference effects might well make the elongated store appear better. A comparison was made between the two DAC shape stores without fins and the standard DAC shape with standard DAC fins (taken from ref. 1), but the standard fins were so small that the increment of drag due to the fins fell within the experimental accuracy.

General store series.- Figure 7(a) gives a comparison of the drag data for four bodies used in various general research programs on external stores. These bodies all have fineness ratios of approximately 10 and pointed afterbodies with the primary differences being in detail shape of the bodies. As will be shown later, the differences in M_{DR} and peak-pressure drag are about what would be expected from the correlation of reference 17 (see figs. 8 and 10) with the exception of M_{DR} for the cylindrical body. The relative subsonic levels of C_D are about what is expected - the NACA 0-series model with the low-fineness-ratio afterbody is high, the cylindrical body with the large wetted area is next, and the NACA 65- and NACA 65A-series bodies agree within the experimental accuracy. The NACA 65A-series bodies showed the reverse trend mentioned earlier.

Low-fineness-ratio series.- Data for three models having fineness ratios of approximately 5 are presented in figure 7(b). The subsonic drag levels for all three agree within the accuracy of the tests, but the M_{DR} for the DAC 10,000-lb-bomb shape appears high in comparison with the other two models. The drag data for the short NACA 65A-series body was not obtained above $M = 1.0$ because of poor radar data in that region.

Nacelle series.- Figure 7(c) presents a comparison of data for nacelle model 1, modification of model 1, and nacelle model 2. Data for nacelle model 1 without a tail plug, that is, with a blunt base, were taken from reference 2. Nacelle model 2 has the same profile in a vertical plane as nacelle model 1 without tail plug, but was designed to be enough wider than nacelle 1 to house two engines side by side. The drag differences between nacelle model 1 and its blunt-base counterpart agree with estimates based on the data of reference 20. The increments between nacelle models 1 and 2 in both M_{DR} and peak-pressure drag agree fairly well with estimates based on the correlation of reference 17. (See figs. 8 and 10.)

Service store series.- Data for models of four service external stores and one modification of the WADC store are compared in figure 7(d). The modified WADC store was simply a standard WADC shape with the elliptic nose replaced by a standard ellipse-plus-cone tail section; the supersonic drag was expected to be reduced with this modification. Again the differences in M_{DR} and peak-pressure drag are about as would be expected except that M_{DR} for the WADC stores appears to be about 0.02 high. The high subsonic C_D of the Navy special store is probably a combined effect of its relatively larger wetted area and the sharp intersection of the conical afterbody and cylindrical midsection.

Drag Correlation

As noted previously, the data from the present series of tests are shown in figures 8 to 10 in terms of the body-drag correlation parameters of reference 17.

Drag-rise Mach number.- The values of M_{DR} originally presented in reference 17 were based on $dC_D/dM = 0.1$; those given in figure 8 for the present tests are based on $dC_D/dM = 1.0$, and the faired curve in figure 8 was taken from a replot of the data used in reference 17 with M_{DR} based on $dC_D/dM = 1.0$. In general, the values of M_{DR} from the present tests agree with data from reference 17 fairly well.

Mach number for peak drag.- Figure 9 shows a comparison of values of the Mach numbers for peak drag from the present tests with those from reference 17. The scatter of data about the faired line is quite large and is several times the scatter shown in reference 17. However, as stated in reference 17, which presented data for parabolic noses only, the Mach number for peak drag depends on nose shape as well as l/d, and the present tests include more blunt-nose shapes where one might expect the scatter in a plot against only fineness ratio to be greater.

Peak-pressure drag.- Values of peak-pressure drag from the present tests are compared with the correlation curve of reference 17 in figure 10. Flagged symbols in figure 10 refer to tests where C_D was still increasing at the maximum test Mach number; peak-pressure drag was based on maximum measured C_D rather than on true maximum C_D. The present data scatter more than those shown in reference 17, and the average value appears to be a little higher than the correlation curve. These effects may be due to the preponderance of blunt-nose shapes among the present models and the fact that a majority of the models in reference 17 had a given base size. In general, however, the present data agree fairly well with the correlation of reference 17.

Friction Drag

No attempt is made to compare the subsonic or friction-drag values for the various models on a quantitative basis because, for several reasons, the accuracy of the present tests does not warrant such comparison. The wide variety of shapes considered required the choice of conservatively large standard fins for the tests. The fin C_D was from 1/4 to 1/2 of the total subsonic C_D. Calculated estimates of body drag were required to determine the fin drag from tests of the fins plus a small body. Also, a variety of construction techniques or material

combinations was required to achieve the proper weights of all the models; and the models were built in small groups and flown at intervals of time over a period of about one year so that it was difficult to maintain consistent surface finish among all the models.

CONCLUDING REMARKS

From the data comparisons and discussion previously presented, it appears that, in general, the shape variations among the several tested store and nacelle shapes had about the expected effects on isolated body drag. Comparison of these data with the body-drag correlation of NACA RM L53I22c showed fairly good agreement in drag-rise Mach number and in peak-pressure drag.

Langley Aeronautical Laboratory,
National Advisory Committee for Aeronautics,
Langley Field, Va., December 3, 1954.

REFERENCES

1. Mitcham, Grady L., and Blanchard, Willard S., Jr.: Low-Lift Drag and Stability Data From Rocket Models of a Modified-Delta-Wing Airplane With and Without External Stores at Mach Numbers From 0.8 to 1.36. NACA RM L53A27, 1953.

2. Pepper, William B., Jr., and Hoffman, Sherwood: Transonic Flight Tests To Compare Zero-Lift Drag of Underslung and Symmetrical Nacelles Varied Chordwise at 40 Percent Semispan of a 45° Sweptback, Tapered Wing. NACA RM L50G17a, 1950.

3. Silvers, H. Norman, King, Thomas J., Jr., and Pasteur, Thomas B., Jr.: Investigation of the Effect of a Nacelle at Various Chordwise and Vertical Positions on the Aerodynamic Characteristics at High Subsonic Speeds of a 45° Sweptback Wing With and Without a Fuselage. NACA RM L51H16, 1951.

4. Spreemann, Kenneth P., and Alford, William J., Jr.: Investigation of the Effects of Geometric Changes in an Underwing Pylon-Suspended External-Store Installation on the Aerodynamic Characteristics of a 45° Sweptback Wing at High Subsonic Speeds. NACA RM L50L12, 1951.

5. Silvers, H. Norman, and King, Thomas J., Jr.: Investigation of the Effect of Chordwise Positioning and Shape of an Underwing Nacelle on the High-Speed Aerodynamic Characteristics of a 45° Sweptback Tapered-In-Thickness-Ratio Wing of Aspect Ratio 6. NACA RM L52K25, 1953.

6. Rainey, Robert W.: Effect of Variations in Reynolds Number on the Aerodynamic Characteristics of Three Bomb or Store Shapes at a Mach Number of 1.62 With and Without Fins. NACA RM L53D27, 1953.

7. Welsh, Clement J., and Morrow, John D.: Effect of Wing-Tank Location on the Drag and Trim of a Swept-Wing Model As Measured in Flight at Transonic Speeds. NACA RM L50A19, 1950.

8. Scallion, William I.: Low-Speed Investigation of the Effects of Nacelles on the Longitudinal Aerodynamic Characteristics of a 60° Sweptback Delta-Wing—Fuselage Combination With NACA 65A003 Airfoil Sections. NACA RM L52F04, 1952.

9. Hoffman, Sherwood, and Pepper, William B., J.: The Effect of Nacelle Combinations and Size on the Zero-Lift Drag of a 45° Sweptback Wing and Body Configuration as Determined by Free-Flight Tests at Mach Numbers Between 0.8 and 1.3. NACA RM L53E25, 1953.

10. Hasel, Lowell E., and Sevier, John R., Jr.: Aerodynamic Characteristics at Supersonic Speeds of a Series of Wing-Body Combinations Having Cambered Wings With an Aspect Ratio of 3.5 and a Taper Ratio of 0.2. Effect at M = 1.60 of Nacelle Shape and Position on the Aerodynamic Characteristics in Pitch of Two Wing-Body Combinations With 47° Sweptback Wings. NACA RM L51K14a, 1952.

11. Muse, T. C., and Bratt, R. W.: Summary of High Speed Wind-Tunnel Tests of a Duglas Aircraft Store Shape and a 2000-Pound G.P.-AN-M66 Bomb. Rep. No. E.S. 21150, Douglas Aircraft Co., Inc., June 25, 1948.

12. Muse, T. C., and Radey, K.: Aerodynamic Characteristics of Several External Store Installations on a Swept-Wing Hypothetical Bomber. Rep. No. ES-15456, Douglas Aircraft Co., Inc., Aug. 16, 1950.

13. Dugan, James C.: External Store Development. Memo. Rep. No. WCNSR-43019-1-1, Wright Air Dev. Center, U. S. Air Force, Aug. 13, 1951.

14. DeLeo, R. V., and Rose, R. E.: Aerodynamic Characteristics of Several External Store Installations on a Swept-Wing Configuration at Transonic Speeds. Res. Rep. No. 89, Univ. of Minnesota Inst. Tech., Dept. Aero. Eng. (Contract Noa(s) 51-1091-C, Buro. Aero.), Apr. 1953.

15. Whitcomb, Richard T.: Recent Results Pertaining to the Application of the "Area Rule." NACA RM L53I15a, 1953.

16. Smith, Norman F., Bielat, Ralph P., and Guy, Lawrence D.: Drag of External Stores and Nacelles at Transonic and Supersonic Speeds. NACA RM L53I23b, 1953.

17. Nelson, Robert L., and Stoney, William E., Jr.: Pressure Drag of Bodies at Mach Numbers up to 2.0. NACA RM L53I22c, 1953.

18. Love, Eugene S.: The Base Pressure at Supersonic Speeds on Two-Dimensional Airfoils and Bodies of Revolution (With and Without Fins) Having Turbulent Boundary Layers. NACA RM L53C02, 1953.

19. Hart, Roger G.: Effects of Stabilizing Fins and a Rear-Support Sting on the Base Pressures of a Body of Revolution in Free Flight at Mach Numbers from 0.7 to 1.3 NACA RM L52E06, 1952.

20. Stoney, William E., Jr.: Some Experimental Effects of Afterbody Shape on the Zero-Lift Drag of Bodies for Mach Numbers Between 0.8 and 1.3. NACA RM L53I01, 1953.

TABLE I.- MODEL ORDINATES

65A-series body		65A-series body		65A-series body		65-series body		0-series body	
Fineness ratio 5.00		Fineness ratio 8.00		Fineness ratio 10.00		Fineness ratio 10.68		Fineness ratio 10.04	
x/l, percent	r/l, percent	x/l, percent	r/l, percent	x/l, percent	r/l, percent	x/l, percent	r/l, percent	x/l, percent	r/l, percent
0	0	0	0	0	0	0	0	0	0
.500	1.539	.500	.960	.500	.760	.500	.720	5.530	1.300
.750	1.849	.750	1.160	.750	.980	.750	.870	9.360	2.100
1.250	2.312	1.250	1.480	1.250	1.180	1.250	1.020	20.200	3.300
2.500	3.126	2.500	2.020	2.500	1.620	2.500	1.520	27.000	3.770
5.000	4.344	5.000	2.720	5.000	2.180	5.000	2.040	42.300	4.390
7.500	5.288	7.500	3.320	7.500	2.660	7.500	2.480	53.400	4.810
10.000	6.080	10.000	3.800	10.000	3.040	10.000	2.850	64.300	4.980
15.000	7.338	15.000	4.580	15.000	3.660	15.000	3.430	69.800	4.920
20.000	8.293	20.000	5.160	20.000	4.120	20.000	3.870	75.400	4.750
25.000	9.012	25.000	5.600	25.000	4.480	25.000	4.200	80.600	4.450
30.000	9.529	30.000	5.920	30.000	4.740	30.000	4.440	86.200	3.980
35.000	9.855	35.000	6.140	35.000	4.920	35.000	4.600	89.000	3.480
40.000	9.997	40.000	6.240	40.000	5.000	40.000	4.680	91.700	2.940
45.000	9.917	45.000	6.220	45.000	4.980	45.000	4.670	94.500	2.160
50.000	9.597	50.000	6.080	50.000	4.860	50.000	4.560	96.300	1.700
55.000	9.022	55.000	5.800	55.000	4.640	55.000	4.340	97.300	1.280
60.000	8.240	60.000	5.380	60.000	4.300	60.000	4.030	100.000	0
65.000	7.275	65.000	4.880	65.000	3.900	65.000	3.650		
70.000	6.237	70.000	4.300	70.000	3.440	70.000	3.220		
75.000	5.197	75.000	3.640	75.000	2.920	75.000	2.730		
80.000	4.157	80.000	2.940	80.000	2.360	80.000	2.200		
85.000	3.119	85.000	2.220	85.000	1.780	85.000	1.660		
90.000	2.078	90.000	1.480	90.000	1.180	90.000	1.110		
95.000	1.039	95.000	.760	95.000	.600	95.000	.570		
100.000	0	100.000	.020	100.000	.020	100.000	.020		
L.E. radius = 1.000		L.E. radius = 0.800 T.E. radius = 0.020		L.E. radius = 0.640 T.E. radius = 0.020		L.E. radius = 0.600			

Cylindrical body		Circular-arc body		Circular-arc body		DAC store		Elongated DAC store	
Fineness ratio 9.33		Fineness ratio 5.00		Fineness ratio 7.00		Fineness ratio 8.57		Fineness ratio 10.93	
x/l, percent	r/l, percent	x/l, percent	r/l, percent	x/l, percent	r/l, percent	x/l, percent	r/l, percent	x/l, percent	r/l, percent
0	0	0	0	0	0	0	0	0	0
.360	.300	2.857	1.457	2.857	1.000	1.944	.946	1.706	.742
1.210	.730	5.714	2.771	5.714	1.943	4.722	2.033	4.142	1.594
3.040	1.440	8.571	3.971	8.571	2.800	7.500	2.869	6.579	2.250
4.870	2.090	11.428	5.057	11.428	3.543	10.278	3.513	9.016	2.754
6.710	2.650	14.286	6.028	14.286	4.257	13.056	4.016	11.453	3.148
8.260	3.070	17.143	6.857	17.143	4.857	15.833	4.416	13.890	3.462
9.150	3.290	20.000	7.600	20.000	5.400	18.611	4.745	16.326	3.720
9.690	3.440	22.857	8.257	22.857	5.857	21.389	5.026	18.463	3.941
10.840	3.700	25.714	8.800	25.714	6.257	24.167	5.272	21.200	4.133
11.990	3.940	28.571	9.228	28.571	6.571	26.944	5.485	23.637	4.300
13.140	4.120	31.428	9.571	31.428	6.828	29.722	5.661	26.074	4.439
14.290	4.300	34.286	9.800	34.286	7.000	32.500	5.785	28.510	4.536
15.440	4.440	37.143	9.943	37.143	7.086	35.278	5.833	30.947	4.574
17.740	4.700	40.000	10.000	40.000	7.143	42.500	5.833	37.283	4.574
20.040	4.920	42.857	9.943	42.857	7.114	49.722	5.833	43.618	4.574
22.340	5.080	45.714	9.914	45.714	7.086	52.500	5.812	55.894	4.574
24.640	5.200	48.571	9.800	48.571	7.000	55.278	5.749	58.331	4.557
26.940	5.300	51.428	9.657	51.428	6.886	58.056	5.646	60.768	4.508
29.240	5.340	54.286	9.457	54.286	6.743	60.833	5.507	63.204	4.427
31.540	5.360	57.143	9.200	57.143	6.571	63.611	5.332	65.641	4.318
61.700	5.360	60.000	8.914	60.000	6.371	66.389	5.125	68.078	4.181
68.690	5.200	62.857	8.571	62.857	6.114	69.167	4.888	70.515	4.078
74.950	4.760	65.714	8.200	65.714	5.857	71.944	4.623	72.952	3.832
81.220	3.940	68.571	7.771	68.571	5.543	74.722	4.334	75.388	3.625
87.480	2.760	71.428	7.314	71.428	5.200	77.500	4.023	77.825	3.398
90.600	2.110	74.286	6.800	74.286	4.282	80.278	3.693	80.262	3.155
93.750	1.420	77.143	6.228	77.143	4.428	83.056	3.347	82.699	2.895
96.890	.720	80.000	5.628	80.000	4.000	85.833	2.989	85.136	2.624
98.440	.360	82.857	4.971	82.857	3.514	88.611	2.620	87.572	2.344
100.000	0	85.714	4.257	85.714	3.028	91.389	2.246	90.009	2.055
		88.571	3.514	88.571	2.486	93.611	1.944	92.446	1.761
		91.428	2.714	91.428	1.914	95.833	1.630	94.395	1.524
		94.286	1.857	94.286	1.314	98.056	1.208	96.345	1.278
		97.143	.943	97.143	.686	100.000	0	98.294	.947
		100.000	0	100.000	0			100.000	0
						T.E. radius = 0.556		T.E. radius = 0.436	

TABLE I.- MODEL ORDINATES - Concluded

DAC 10,000-lb bomb		WADC Store		Modified WADC store		Navy special 1A-2000 lb store		F-84 tank	
Fineness ratio 5.10		Fineness ratio 7.78		Fineness ratio 8.78		Fineness ratio 8.57		Fineness ratio 7.43	
x/l, percent	r/l, percent	x/l, percent	r/l, percent	x/l, percent	r/l, percent	x/l, percent	r/l, percent	x/l, percent	r/l, percent
0	0	0	0	0	0	0	0	0	0
.209	.934	.385	1.110	5.693	1.275	1.561	1.926	.384	.522
.418	1.329	.899	1.683	11.386	2.550	3.818	3.100	1.153	.933
1.040	2.126	1.285	2.004	18.981	4.247	6.169	4.074	1.922	1.234
2.093	3.037	1.606	2.236	22.772	4.930	8.596	4.839	3.848	1.829
5.233	4.847	3.212	3.109	28.465	5.511	11.080	5.390	7.696	2.746
10.466	6.763	6.424	4.253	34.158	5.693	13.602	5.722	12.928	3.695
15.702	8.022	8.570	4.793	65.842	5.693	16.144	5.833	19.230	4.718
20.933	8.864	12.849	5.564	71.535	5.511	72.812	5.833	23.088	5.214
26.166	9.396	19.274	6.219	77.228	4.930	78.367	4.641	26.922	5.631
31.399	9.689	25.698	6.424	81.019	4.247	83.923	3.448	30.783	5.982
37.500	9.795	61.452	6.424	88.614	2.550	89.478	2.258	34.613	6.265
42.671	9.720	67.877	6.219	94.307	1.275	95.034	1.066	38.461	6.478
47.842	9.498	74.302	5.564	100.000	0	100.000	0	42.304	6.631
53.013	9.128	78.580	4.793					48.078	6.733
48.184	8.615	87.151	2.878			L.E. radius = 1.750		50.000	6.728
63.355	7.967	93.575	1.439					57.719	6.552
68.526	7.194	100.000	0					65.382	6.089
73.697	6.308							73.111	5.320
78.868	5.326							76.922	4.820
84.173	4.246							80.807	4.241
89.210	3.150							84.613	3.575
94.381	2.001							88.502	2.820
99.254	.914							92.350	1.973
100.000	0							96.198	1.033
								98.125	.528
L.E. radius = 2.016								100.000	0
T.E. radius = 0.933								L.E. radius = 0.007	
								T.E. radius = 0.001	

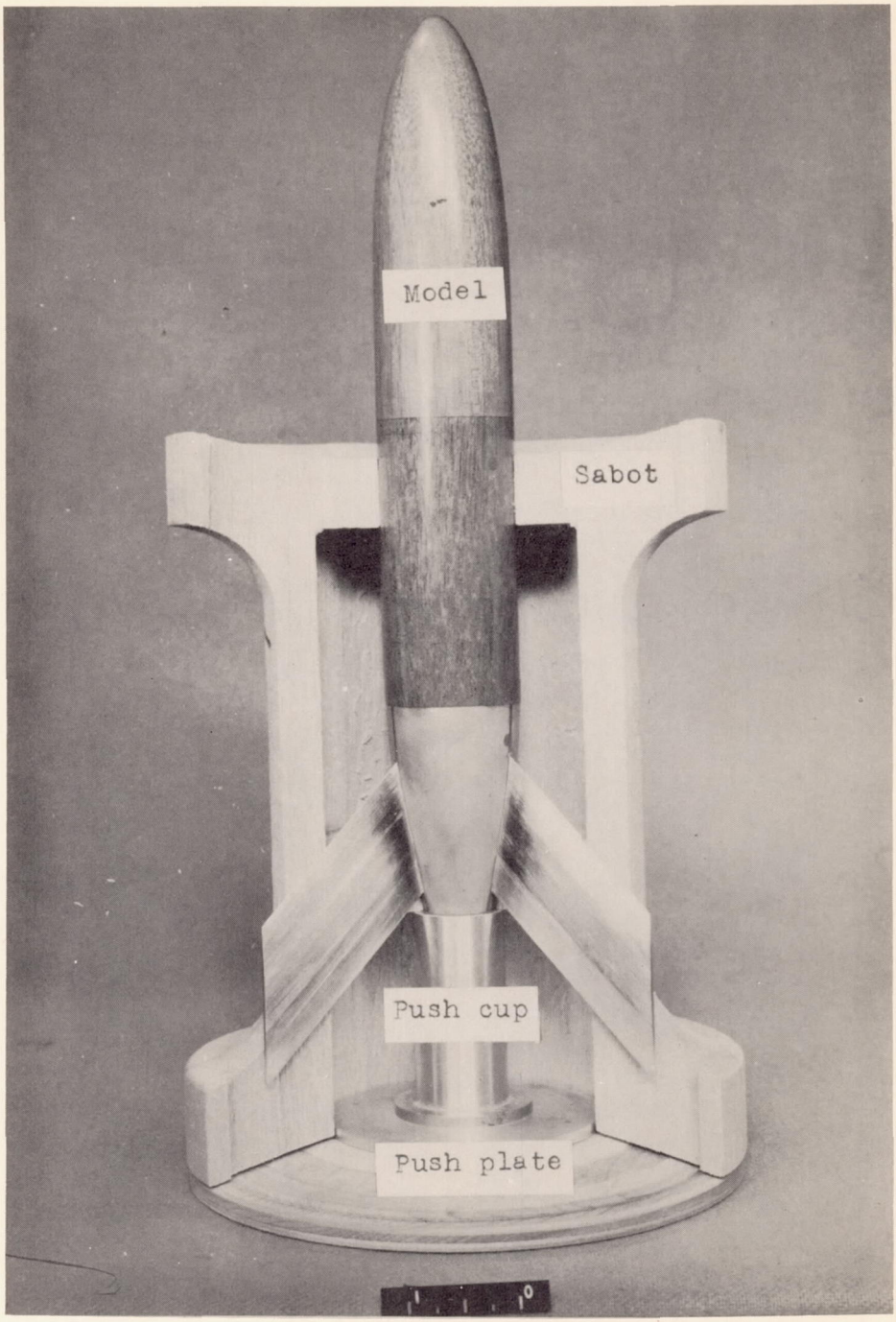
F-94 tank		Nacelle model 1		Nacelle model 2		Nacelle model 3		Nacelle model 4	
Fineness ratio 7.15		Fineness ratio 11.08		Fineness ratio 6.40		Fineness ratio 9.51		Fineness ratio 8.81	
x/l, percent	r/l, percent	x/l, percent	r/l, percent	x/l, percent	r/l, percent	x/l, percent	r/l, percent	x/l, percent	r/l, percent
0	0	0	0	0	0	0	0	0	0
3.594	2.614	.360	.252	.412	.289	7.008	2.011	7.416	1.987
6.693	4.022	1.186	.608	1.361	.697	10.512	2.957	11.206	2.958
11.243	5.374	2.984	1.208	3.423	1.386	14.015	3.756	12.500	3.219
14.969	6.100	4.782	1.758	5.484	2.016	17.519	4.387	14.479	3.604
19.387	6.660	6.579	2.236	7.546	2.565	21.023	4.856	16.667	3.954
28.289	6.990	8.377	2.686	9.608	3.080	24.527	5.151	22.917	4.766
60.435	6.990	9.276	2.876	10.639	3.299	28.031	5.256	29.167	5.275
67.491	6.792	10.635	3.150	12.198	3.612	71.969	5.256	36.417	5.566
78.371	5.044	12.889	3.502	14.783	4.016	75.473	5.151	40.208	5.637
89.614	2.539	17.401	3.973	19.959	4.557	78.977	4.856	45.833	5.673
100.000	0	21.913	4.278	25.134	4.907	82.481	4.387	52.083	5.656
		26.425	4.458	30.309	5.113	85.985	3.756	58.333	5.619
		30.938	4.512	35.484	5.175	89.488	2.951	64.583	5.523
		60.509	4.512	69.402	5.175	92.992	2.011	70.833	5.350
		64.255	4.447	73.699	5.101	100.000	0	77.083	5.116
		67.998	4.296	77.992	4.928			83.333	4.750
		71.744	4.052	82.289	4.647			89.583	4.296
		75.487	3.700	86.581	4.243			95.833	3.710
		79.233	3.268	90.878	3.748			100.000	3.255
		82.976	2.761	95.171	3.167				
		86.722	2.215	99.468	2.540				
		87.186	2.150	100.000	2.466				
		93.593	1.075						
		100.000	0	L.E. radius = 0.206					
		L.E. radius = 0.180							

TABLE II.- AN INDEX OF BODY SHAPES, FINENESS RATIOS, AND SOURCES

Figure	Body shape	Fineness ratio, l/d	Reference
5(a)	NACA 65A series	5.00	3
5(b)	NACA 65A series	8.00	4
5(c)	NACA 65A series	10.00	4
5(d)	NACA 65 series	10.68	5
5(e)	NACA 0 series	10.04	5
5(f)	Cylindrical	9.33	5
5(g)	Circular arc	5.00	6
5(h)	Circular arc	7.00	6
5(i)	DAC store[1]	8.57	11
5(j)	Elongated DAC store	10.93	Unpublished
5(k)	DAC 10,000-lb bomb	5.10	12
5(l)	WADC store[2]	7.78	13
5(m)	Modified WADC store	8.78	Unpublished
5(n)	Navy special 1A-2000 lb store	8.57	14
5(o)	F-84 tank	7.43	7
5(p)	F-94 tank	7.15	Unpublished
5(q)	Nacelle 1	11.08	8
5(r)	Nacelle 2	6.40	9
5(s)	Nacelle 3	9.51	10
5(t)	Nacelle 4	8.81	Unpublished

[1]Douglas Aircraft Company.

[2]Wright-Air Development Center.



L-79485.1

Figure 1.- Typical model, push plate, push cup, and sabot with one section removed.

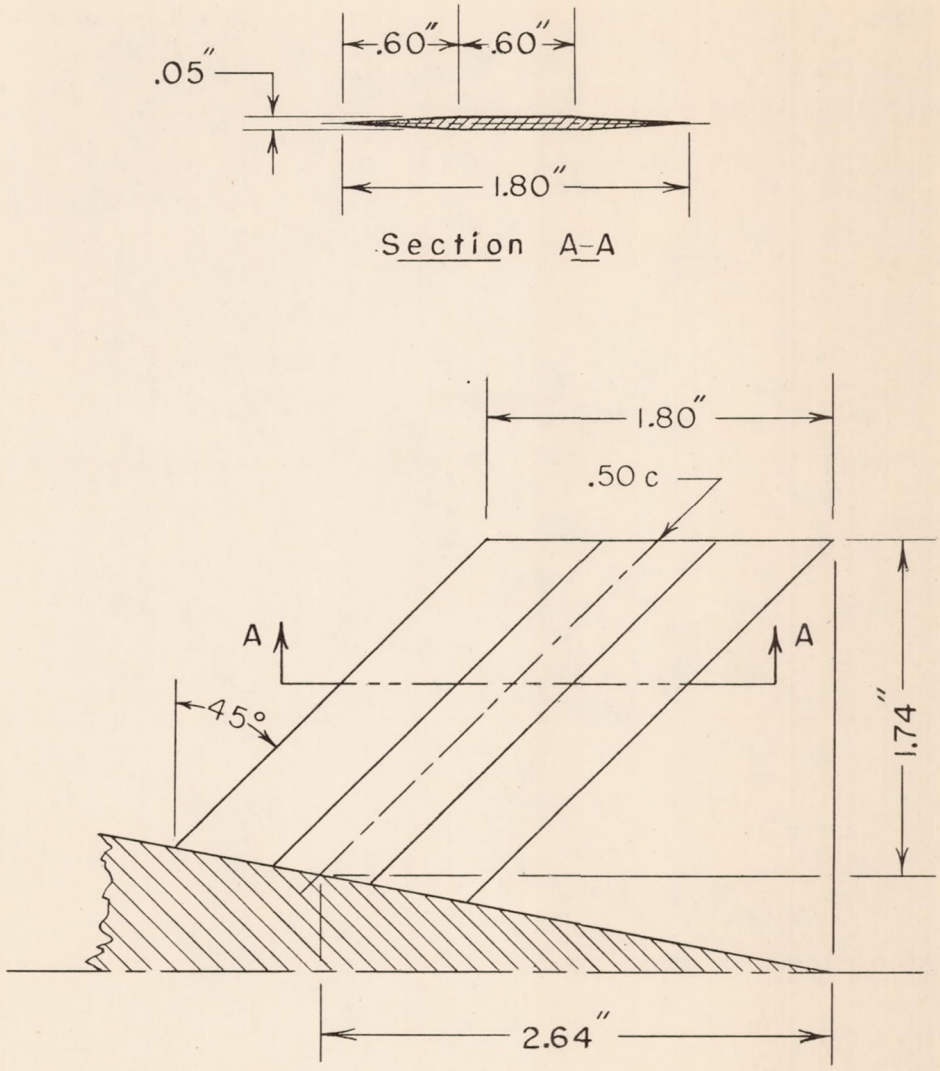
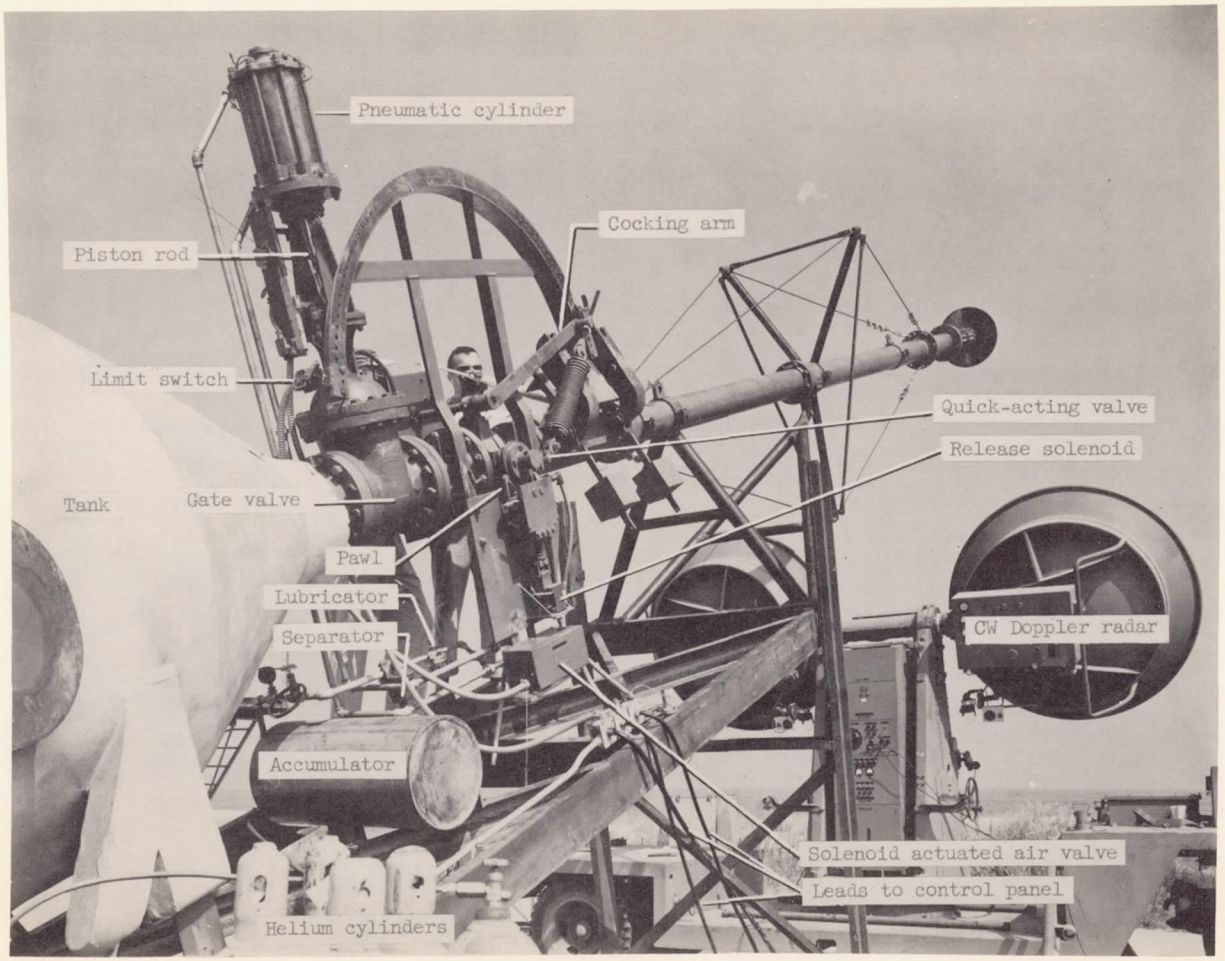
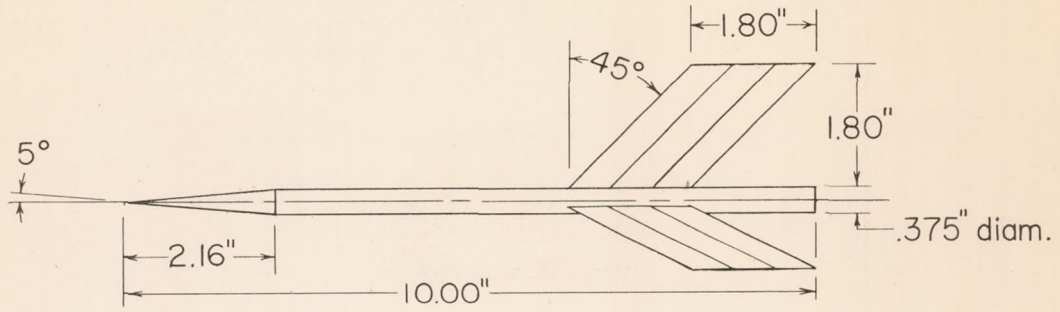


Figure 2.- Sketch of typical model stabilizing fin.

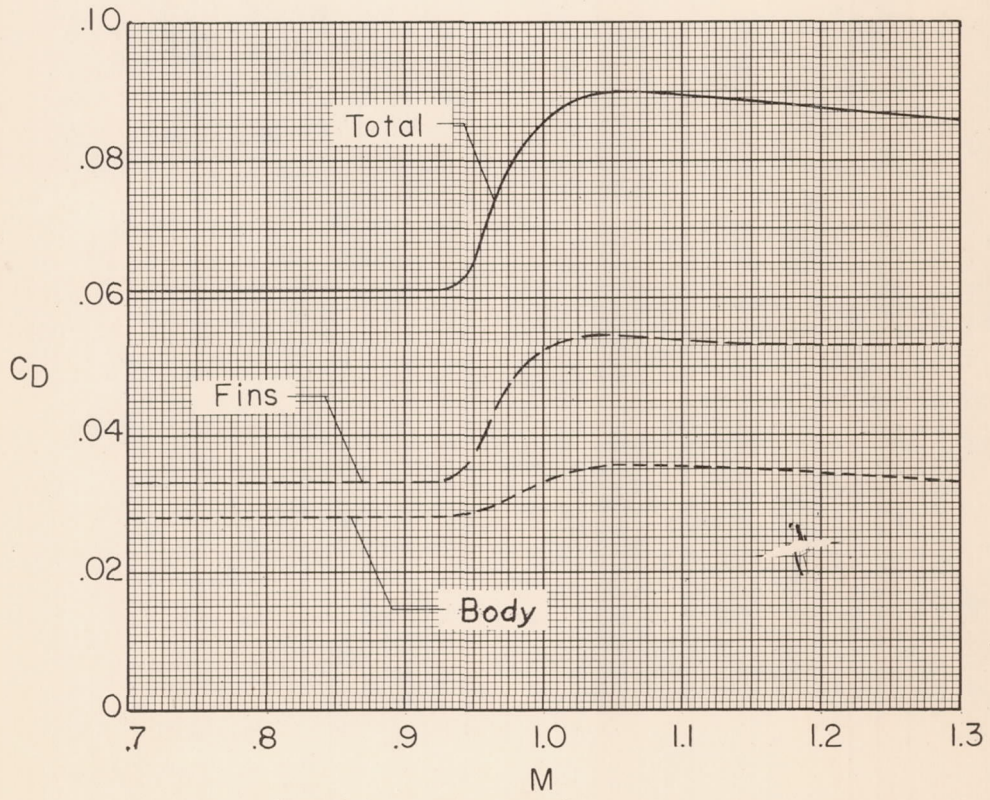


L-66870.1

Figure 3.- General view of helium gun mechanism with CW Doppler radar set in tracking position.

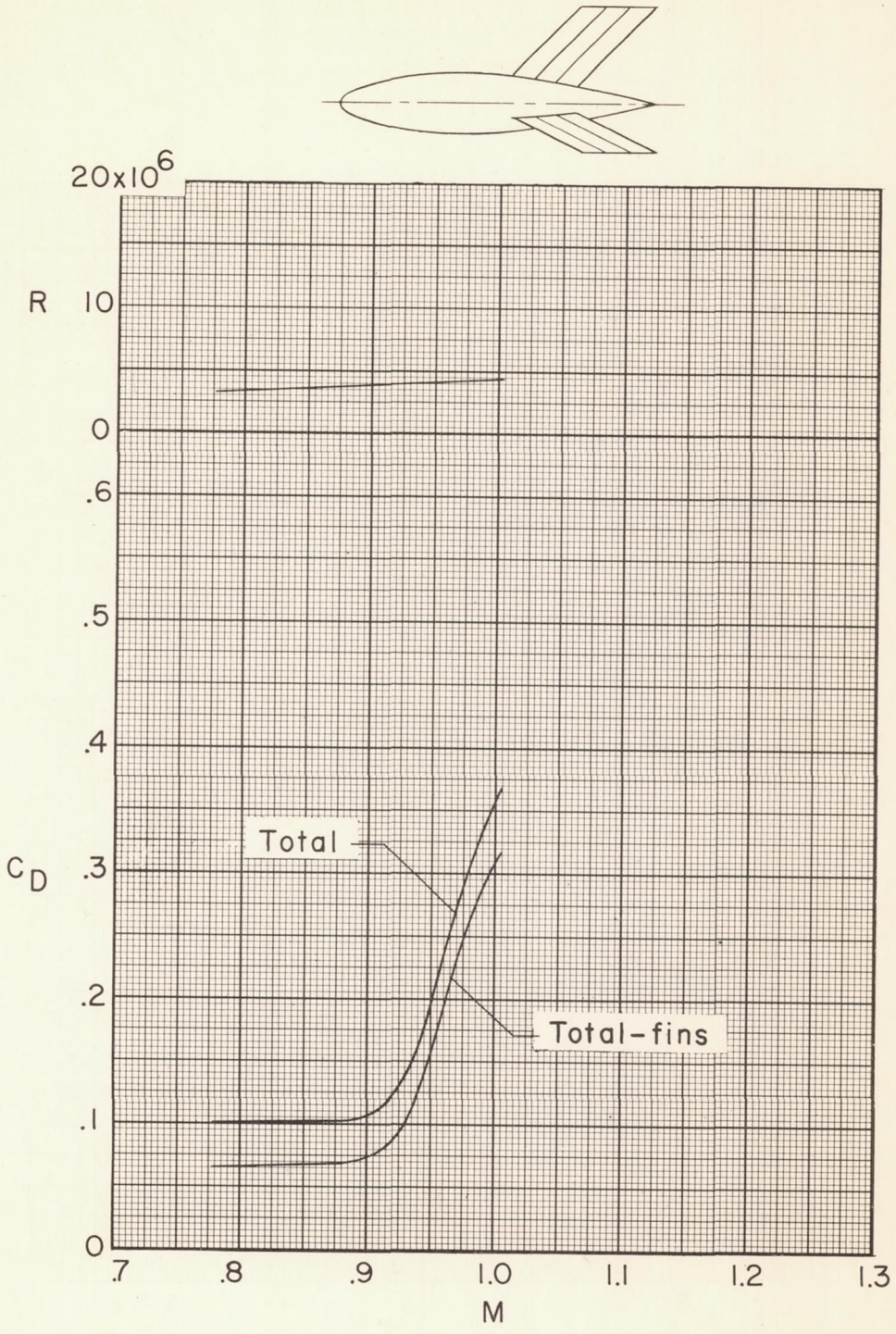


(a) Sketch of fin-drag test model.



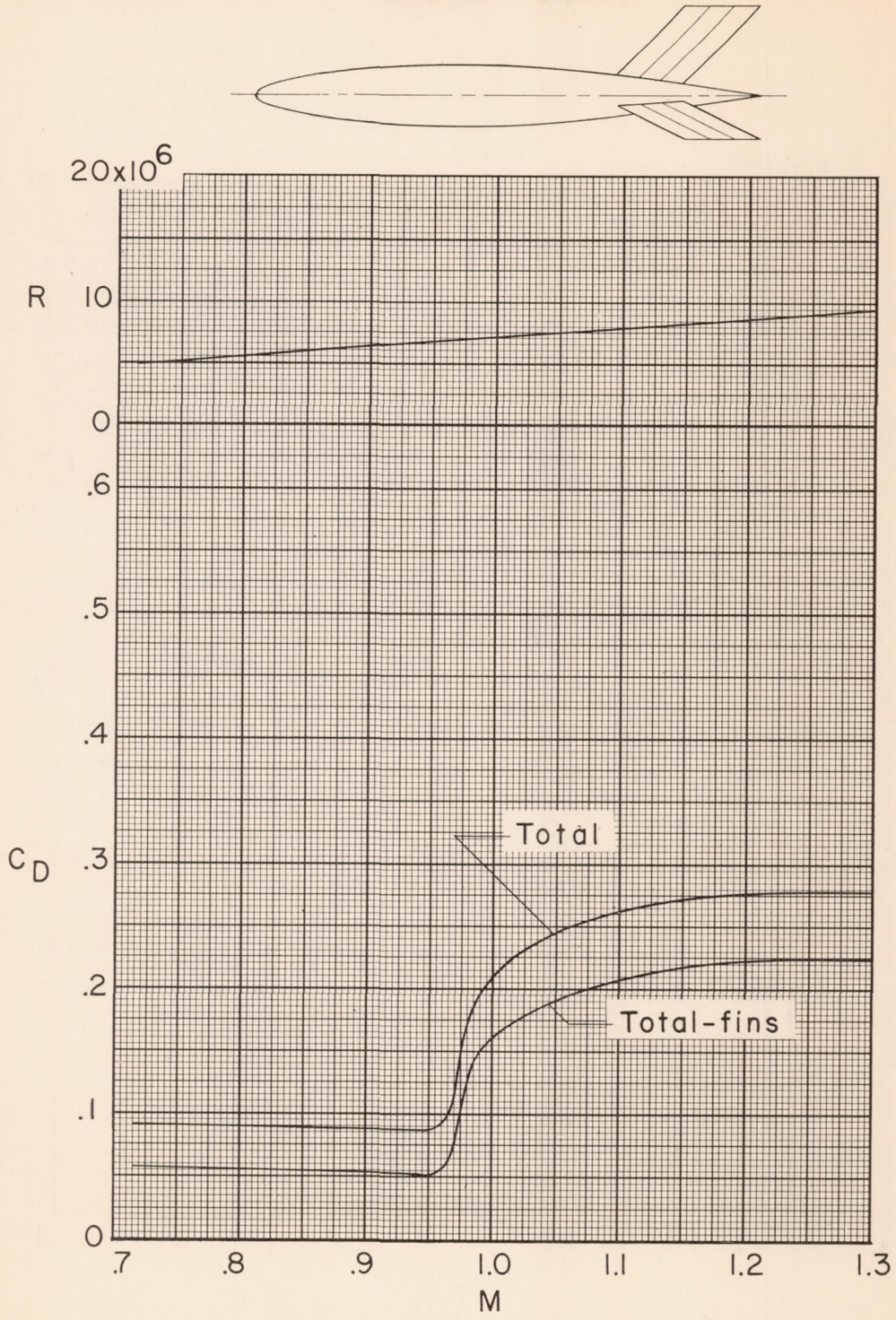
(b) Drag-coefficient data (based on store frontal area of 0.0123 sq ft) as functions of Mach number.

Figure 4.- Fin-drag test model and fin-drag data.



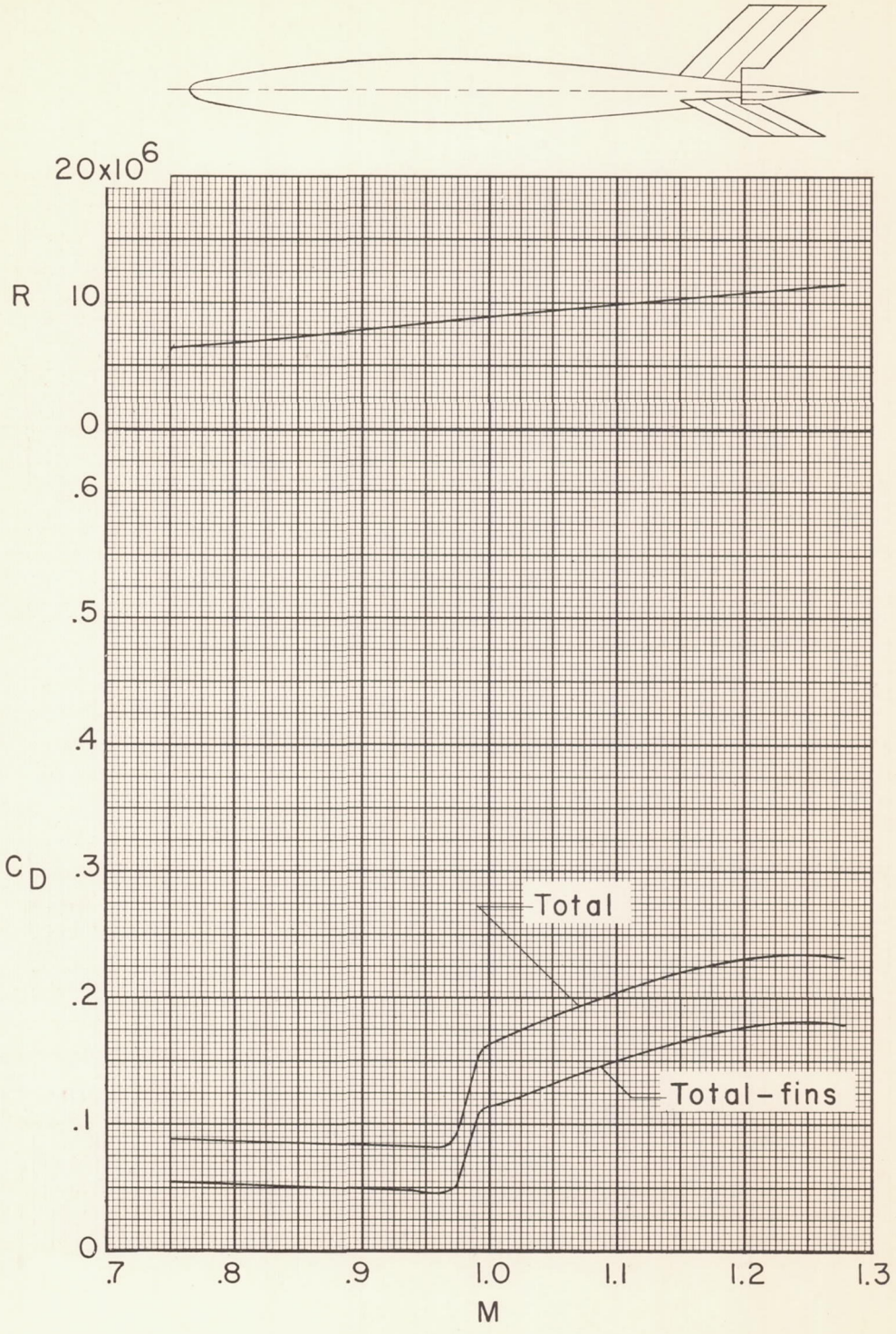
(a) NACA 65A-series body (l/d = 5.00).

Figure 5.- Model sketches with Reynolds number and drag-coefficient data as functions of Mach number (C_D based on store frontal area of 0.0123 sq ft).



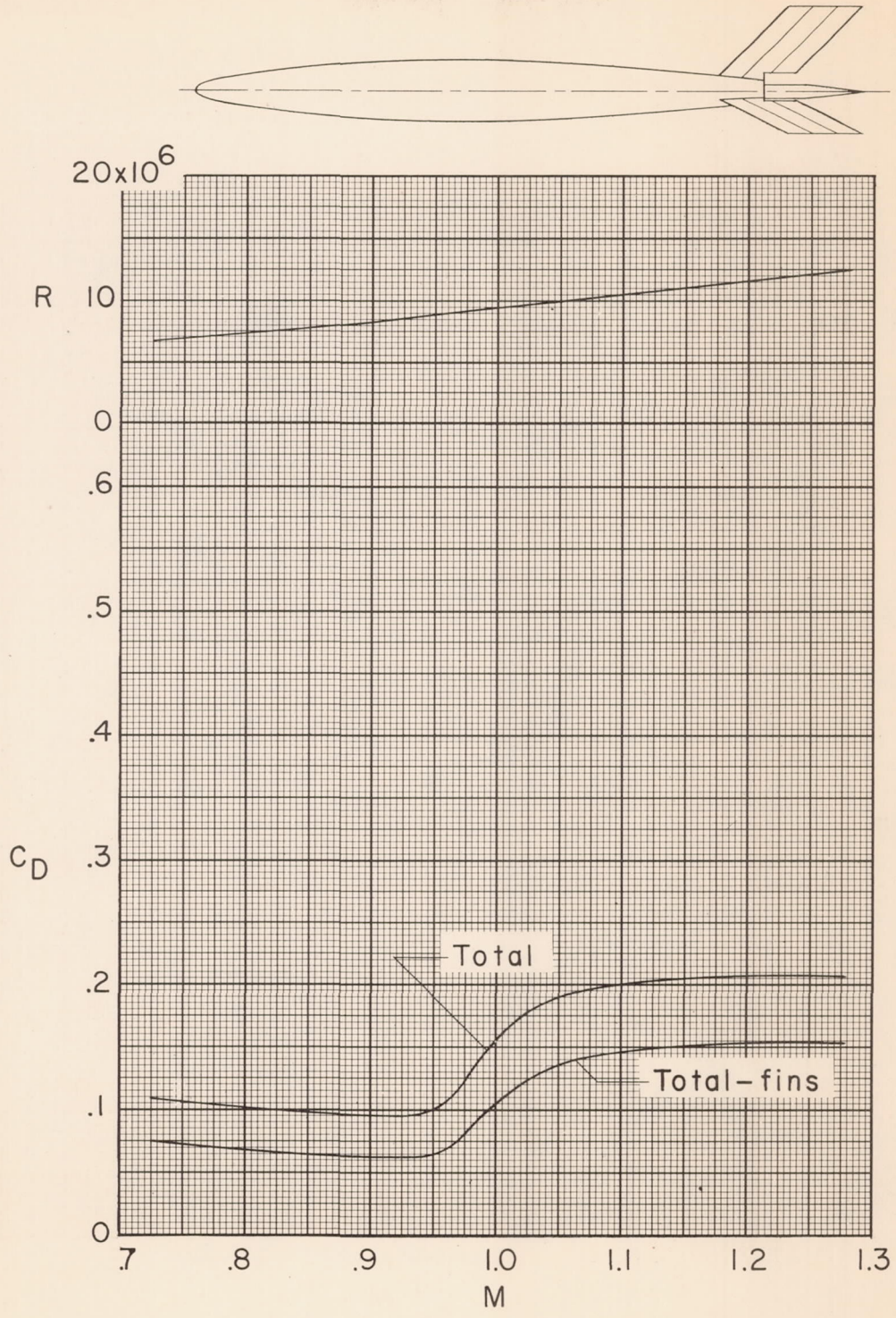
(b) NACA 65A-series body (l/d = 8.00).

Figure 5.- Continued.



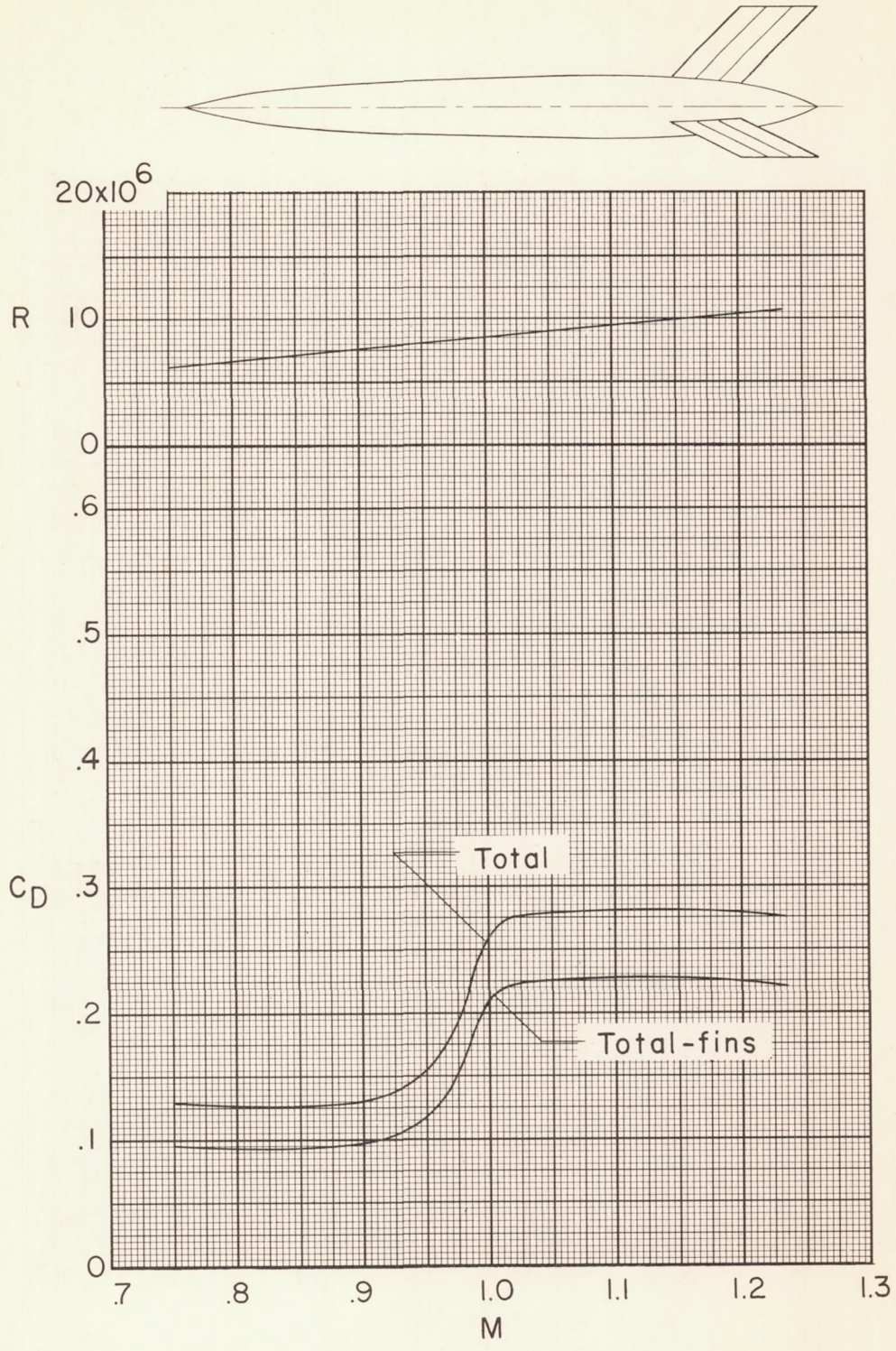
(c) NACA 65A-series body (l/d = 10.00).

Figure 5.- Continued.



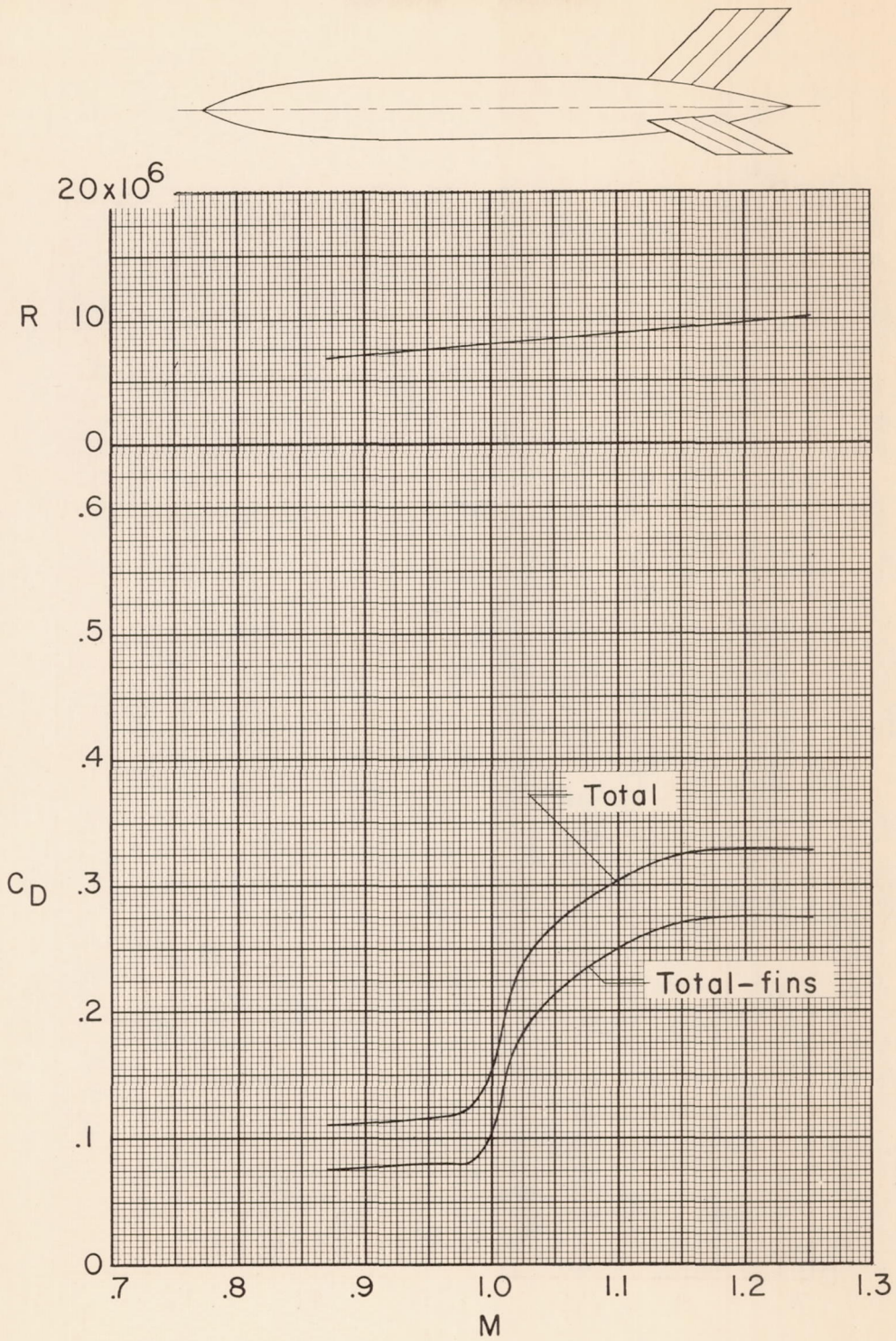
(d) NACA 65-series body (l/d = 10.68).

Figure 5.- Continued.



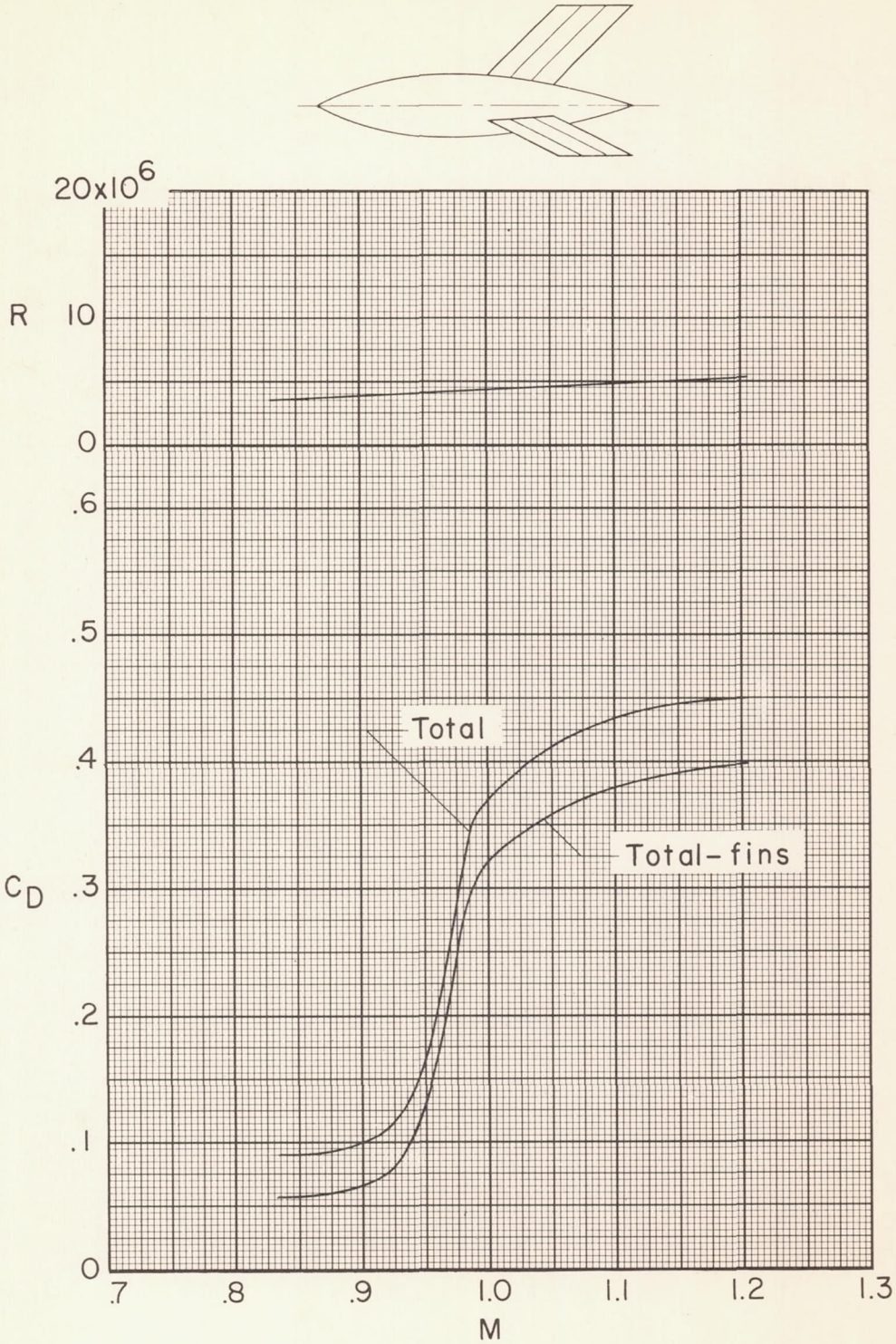
(e) NACA 0-series body (l/d = 10.04).

Figure 5.- Continued.



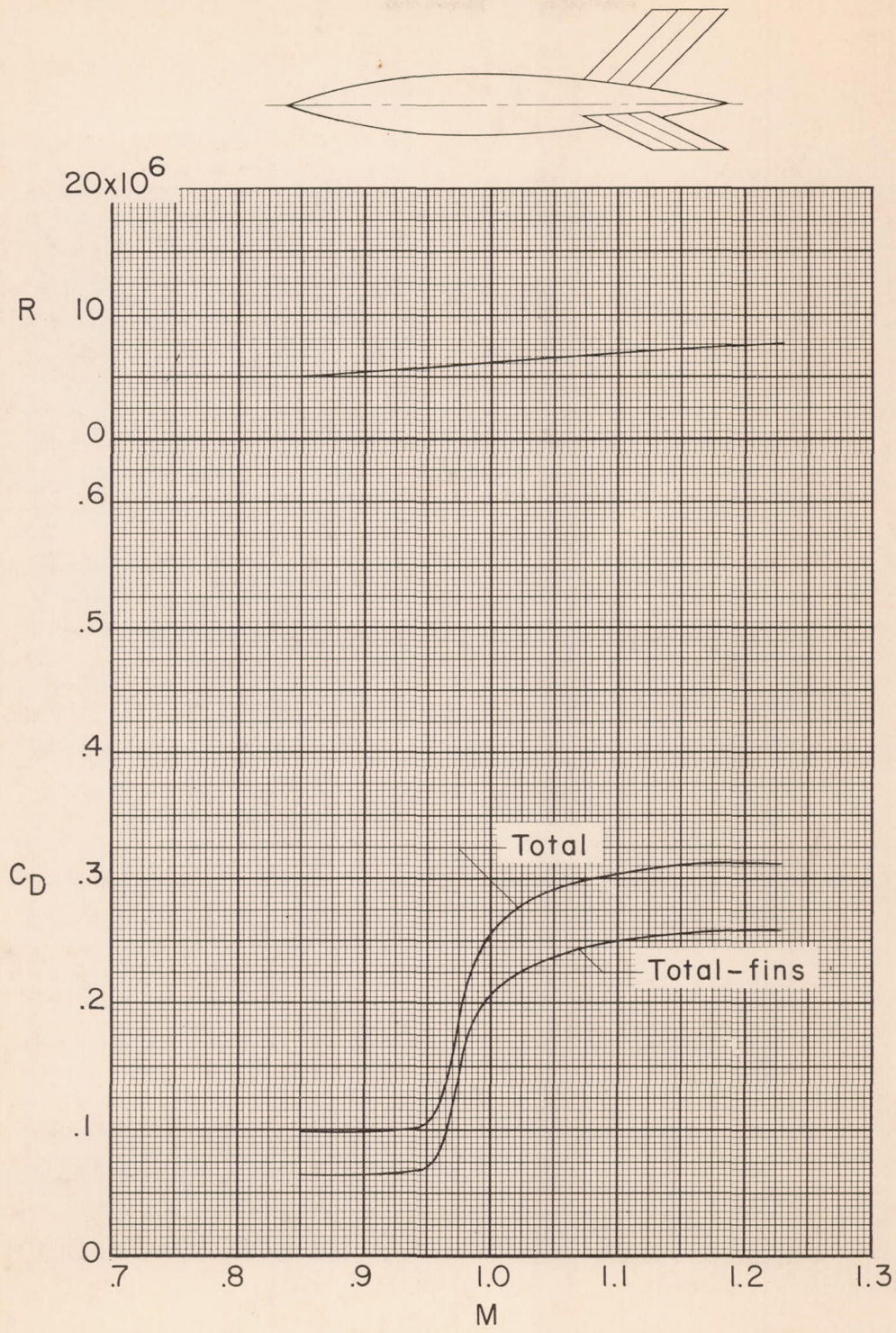
(f) Cylindrical body (l/d = 9.33).

Figure 5.- Continued.



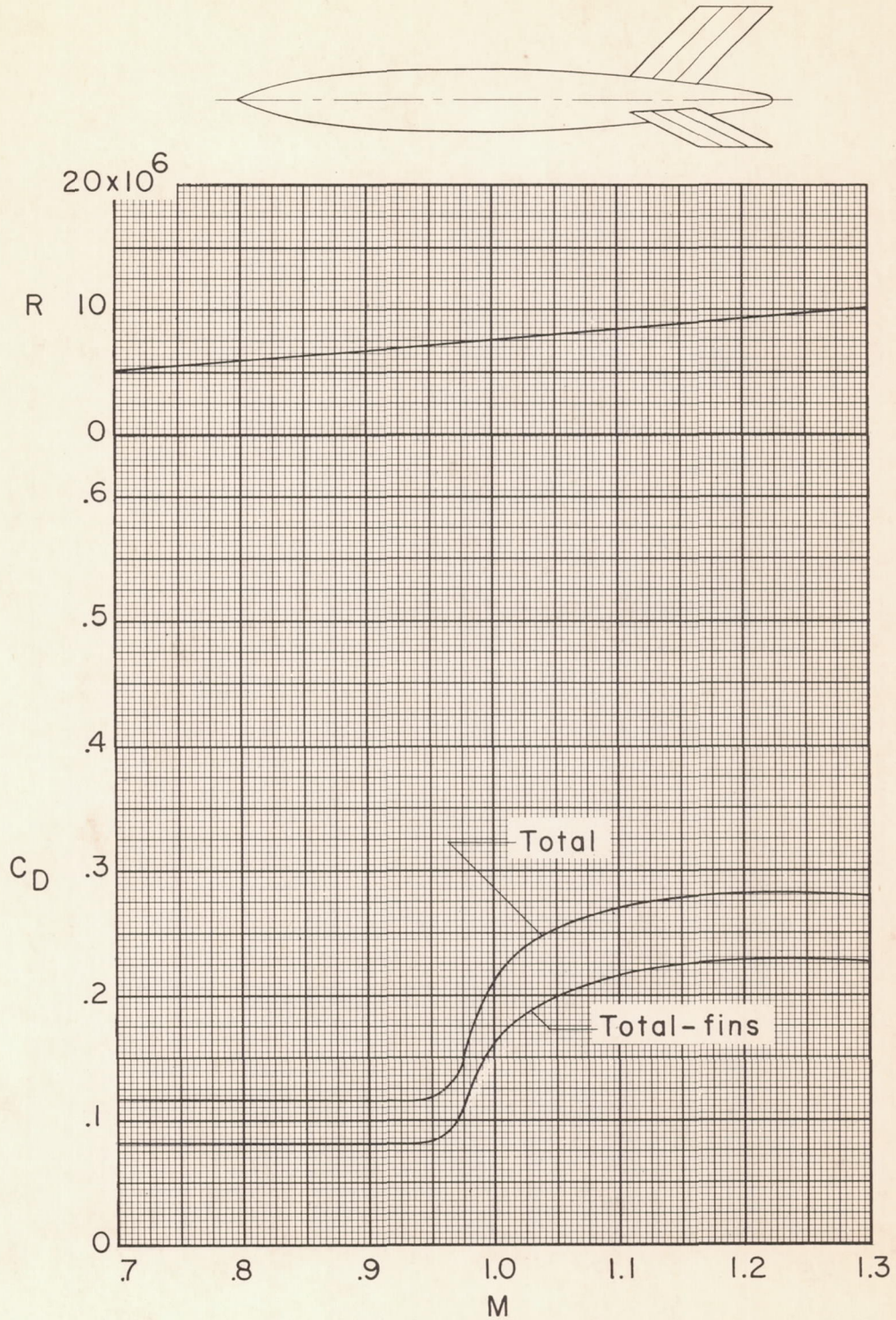
(g) Circular-arc body (l/d = 5.00).

Figure 5.- Continued.



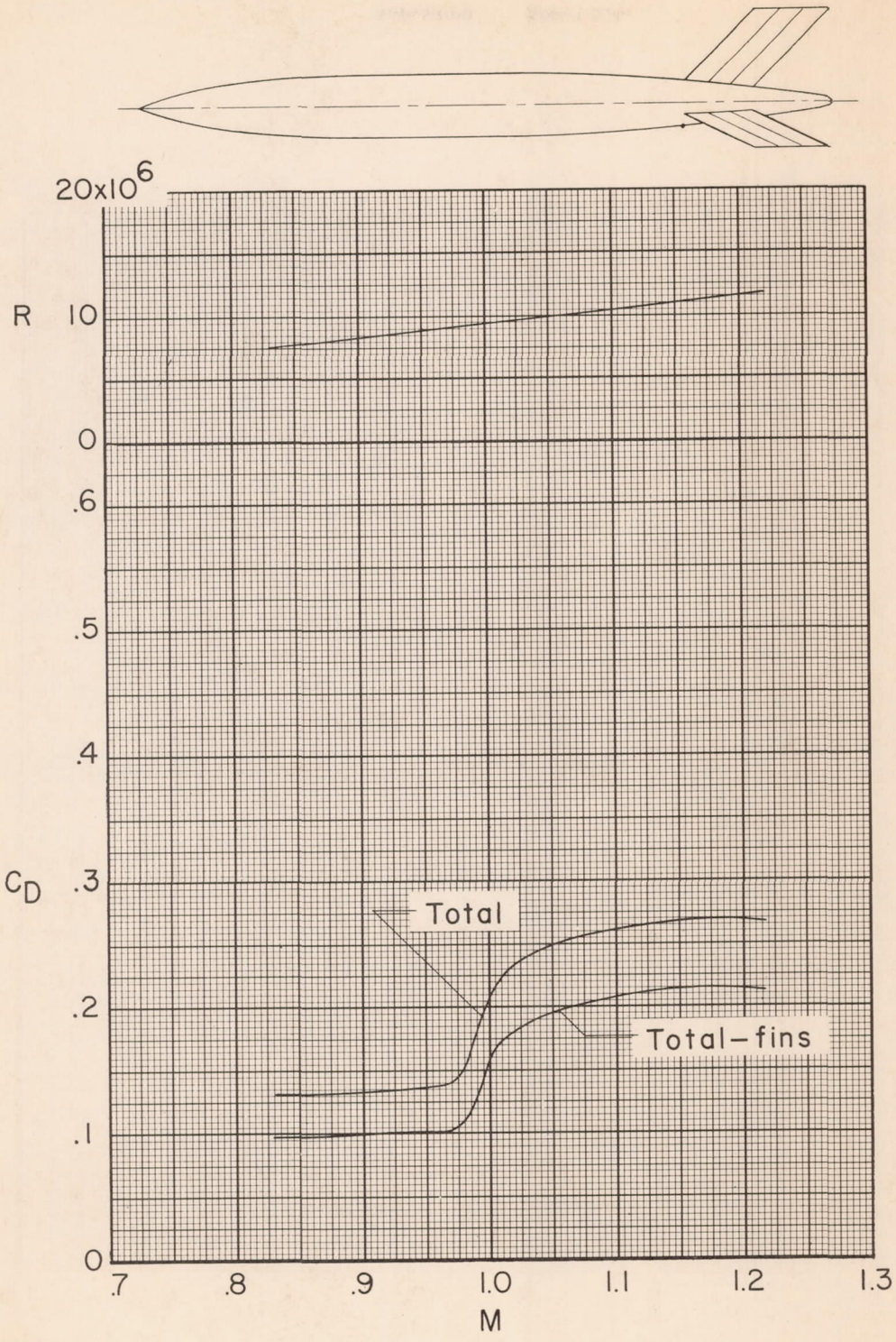
(h) Circular-arc body (l/d = 7.00).

Figure 5.- Continued.



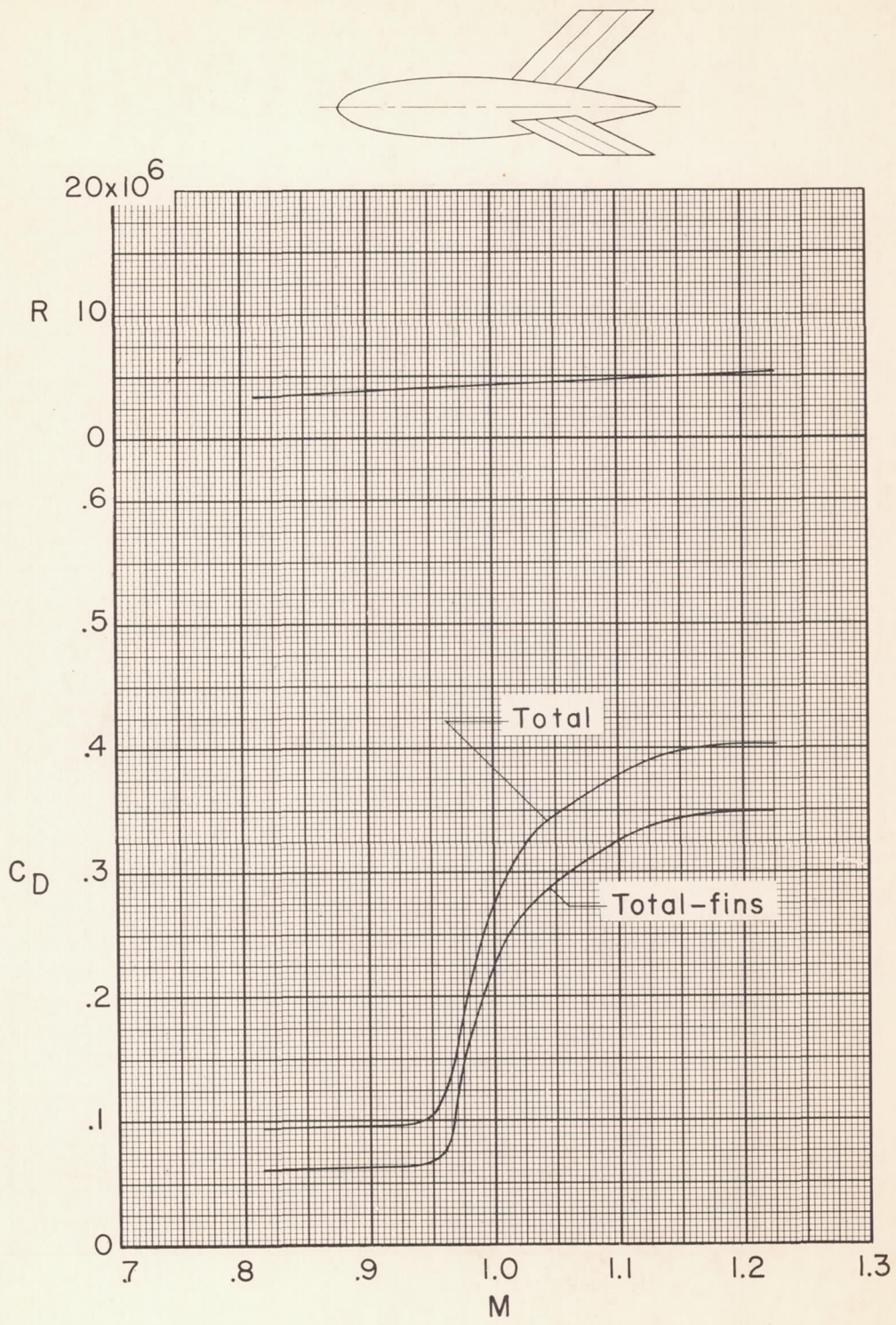
(i) DAC store shape (l/d = 8.57).

Figure 5.- Continued.



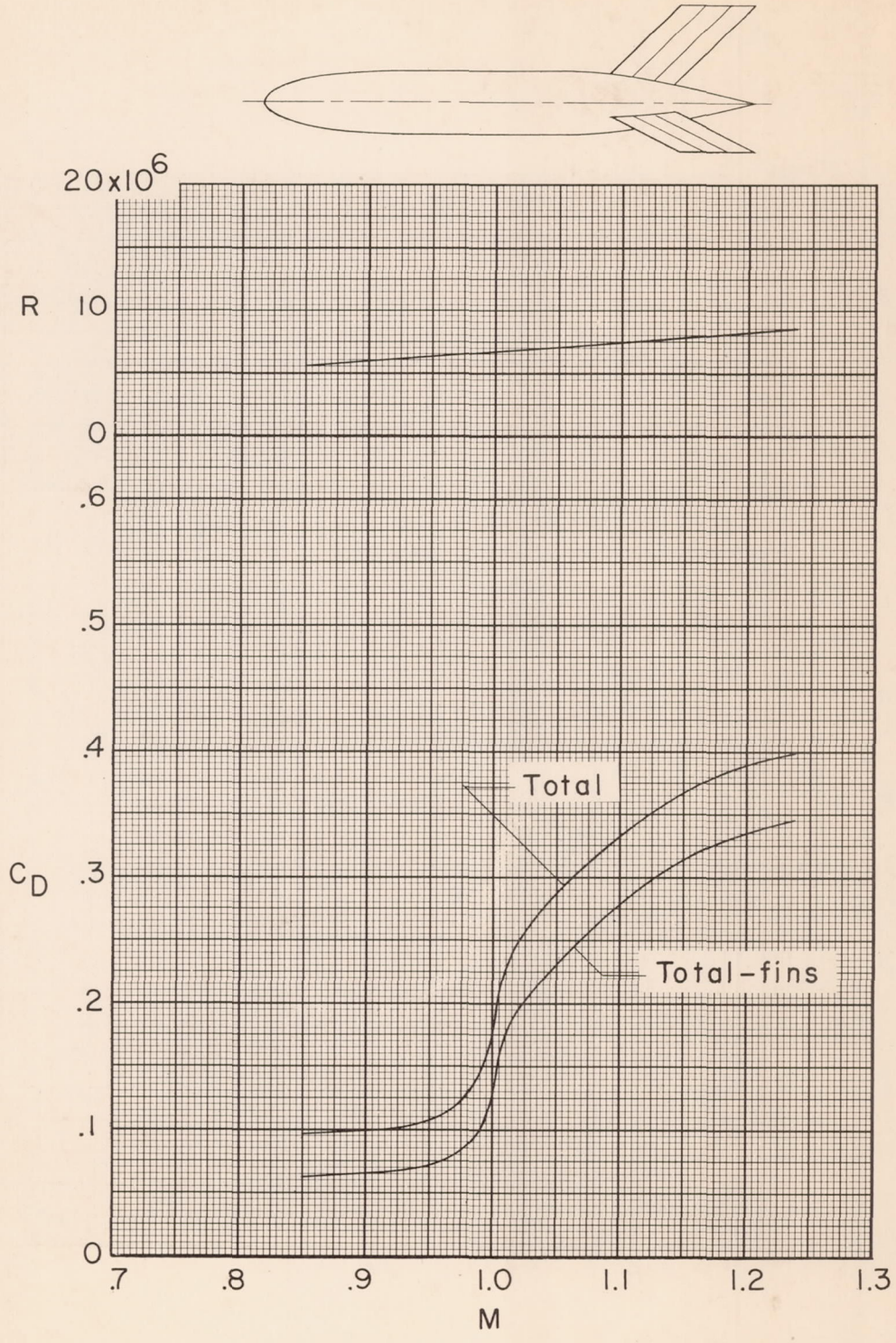
(j) Elongated DAC store shape (l/d = 10.93).

Figure 5.- Continued.



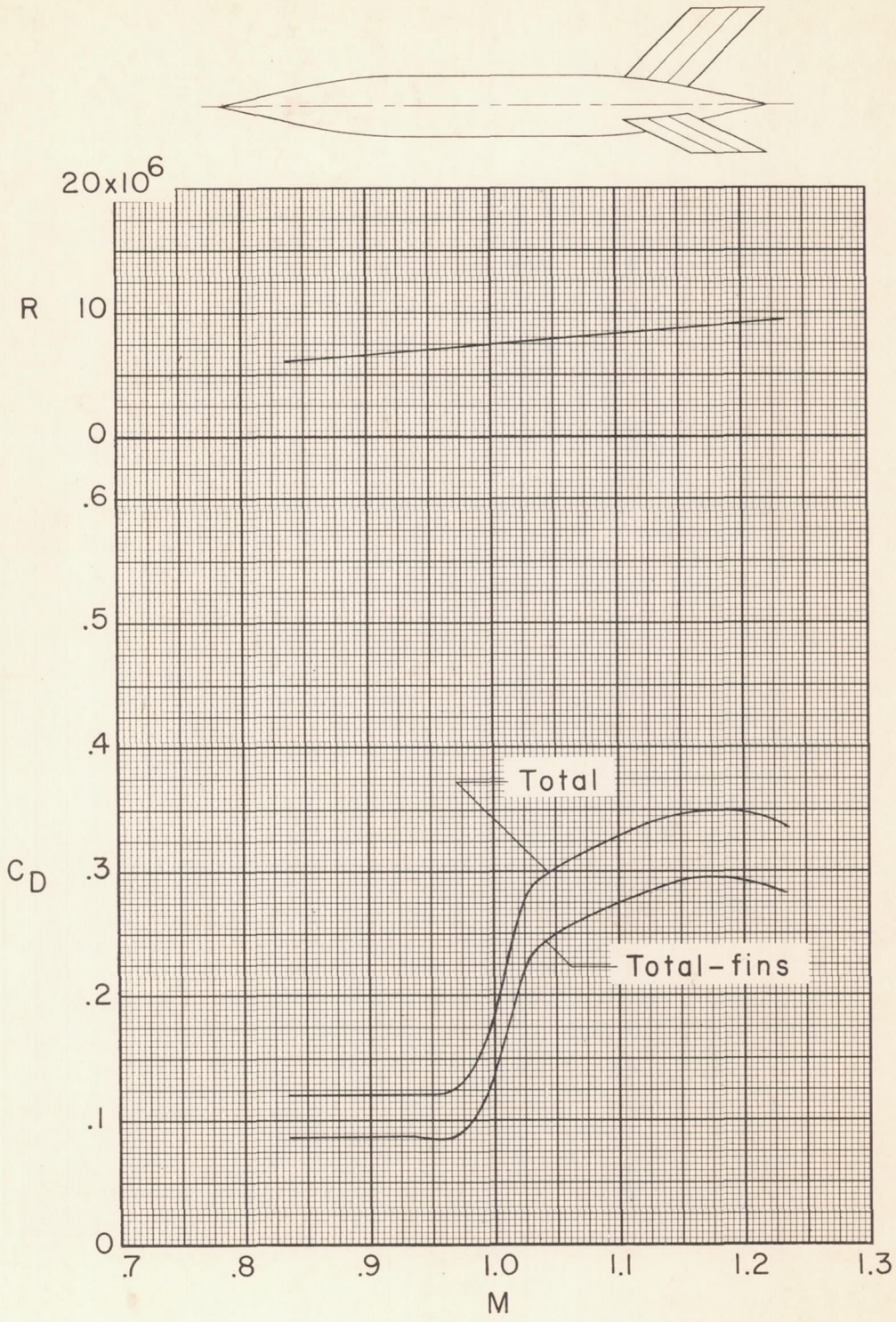
(k) DAC 10,000-lb bomb shape (l/d = 5.10).

Figure 5.- Continued.



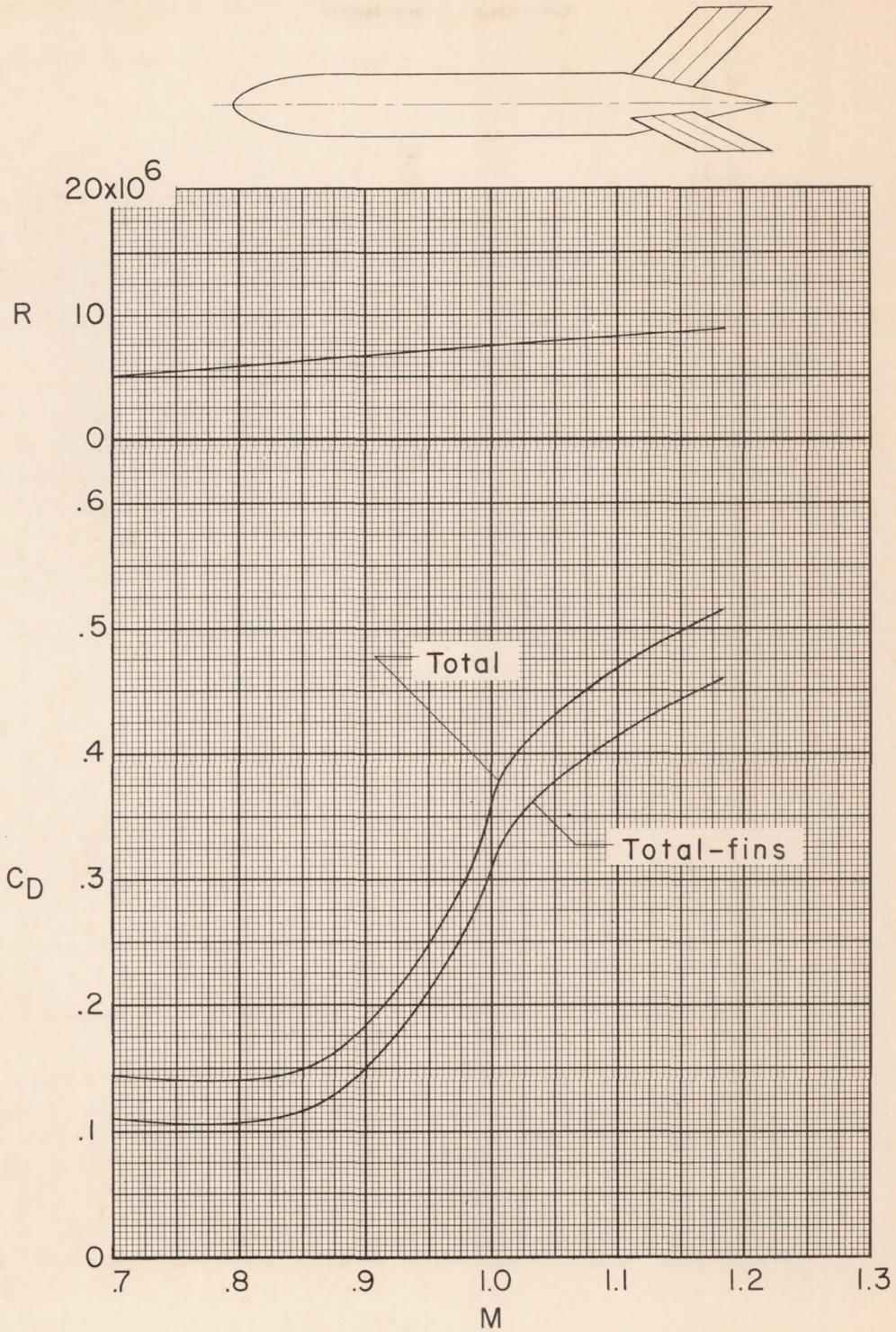
(l) WADC store (l/d = 7.78).

Figure 5.- Continued.



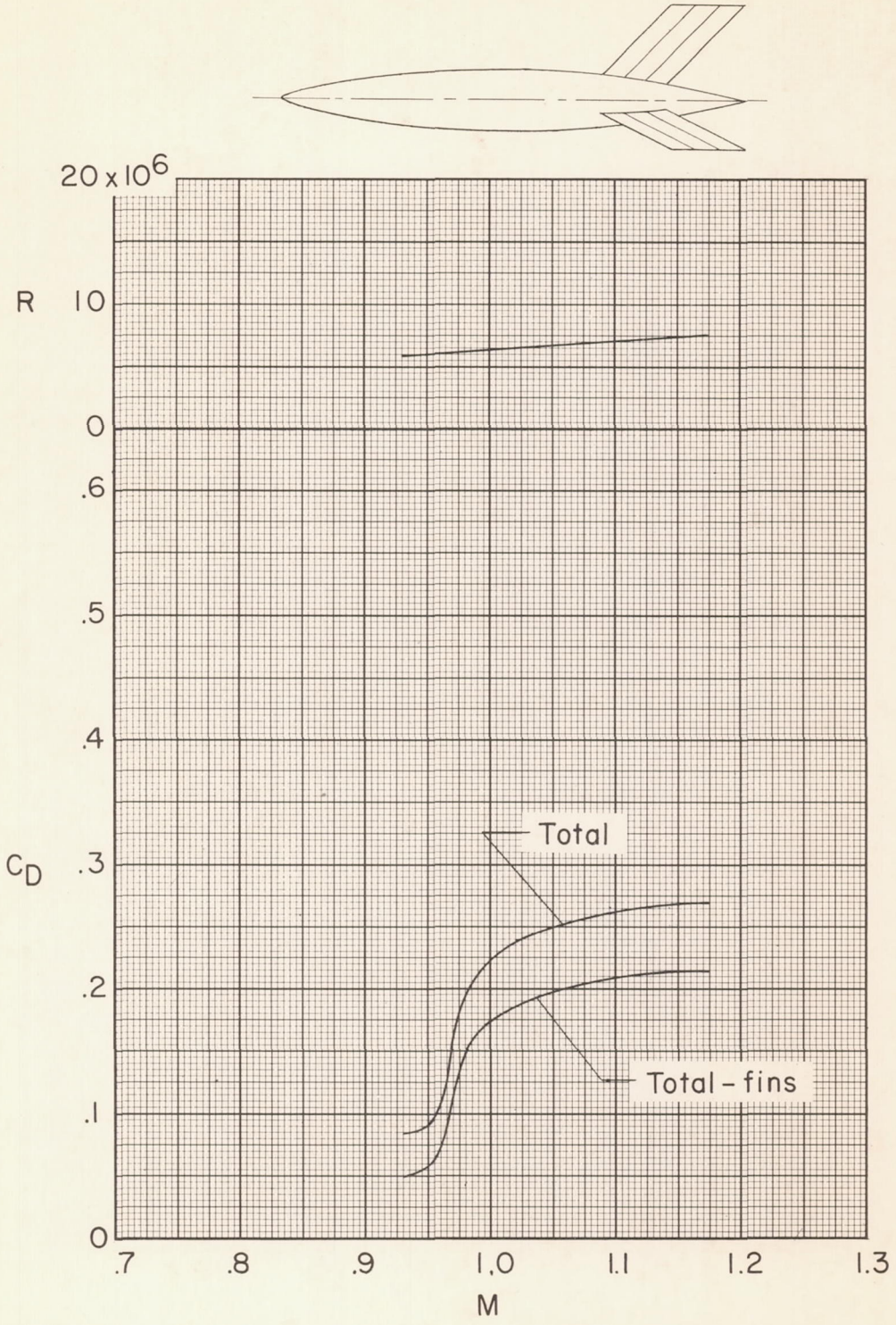
(m) Modified WADC store (l/d = 8.78).

Figure 5.- Continued.



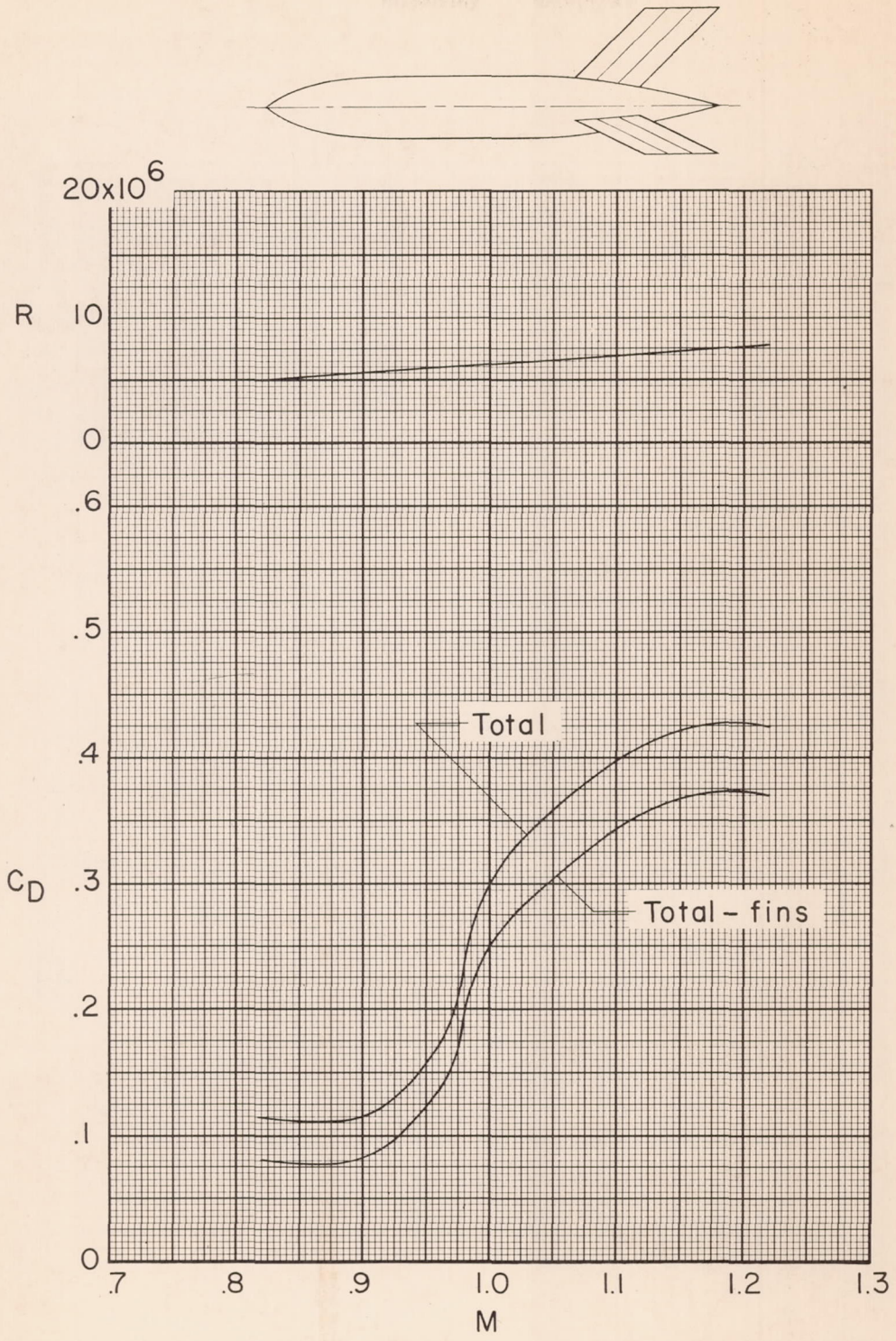
(n) Navy special 1A-2000 lb store (l/d = 8.57).

Figure 5.- Continued.



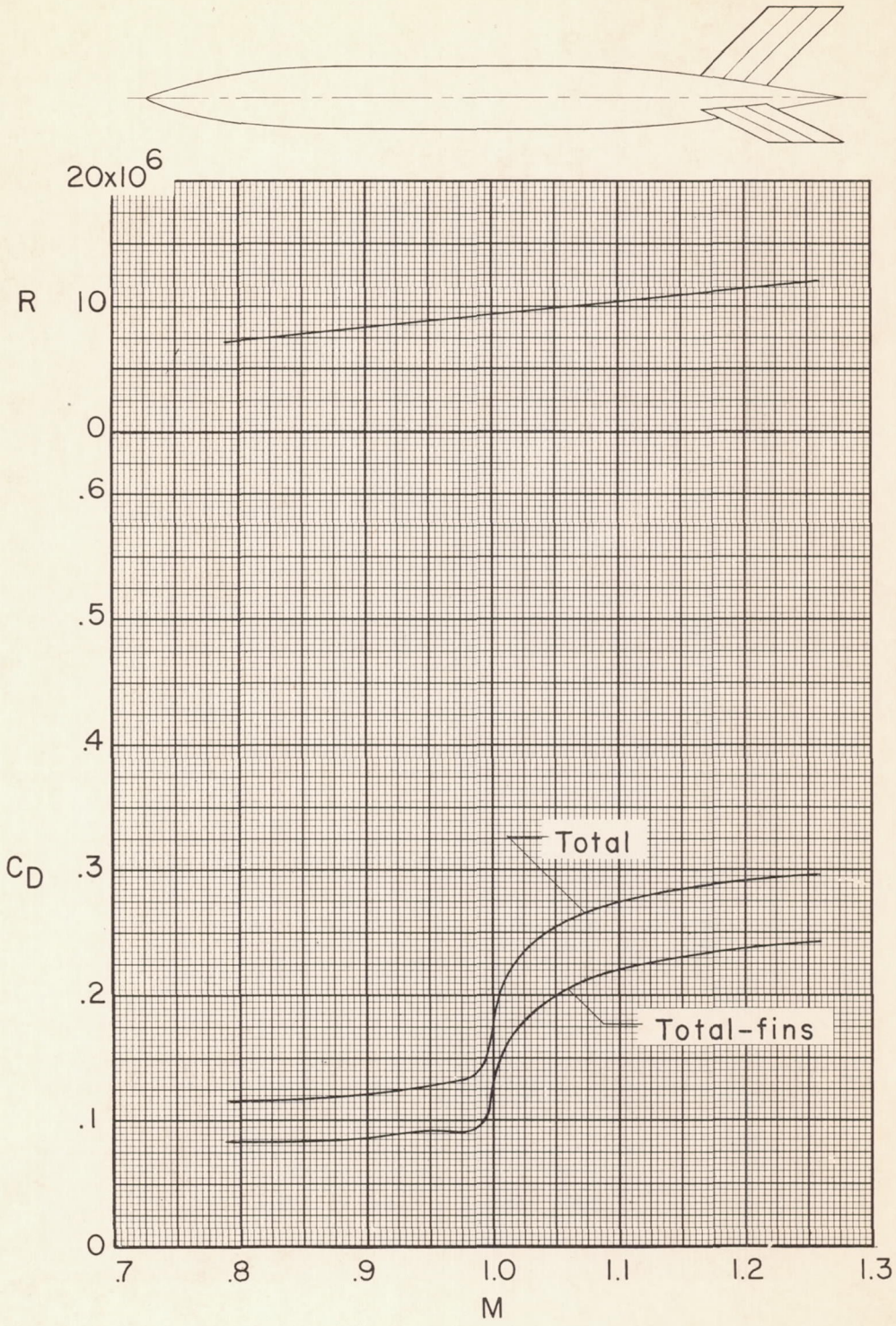
(o) F-84 tank (l/d = 7.43).

Figure 5.- Continued.



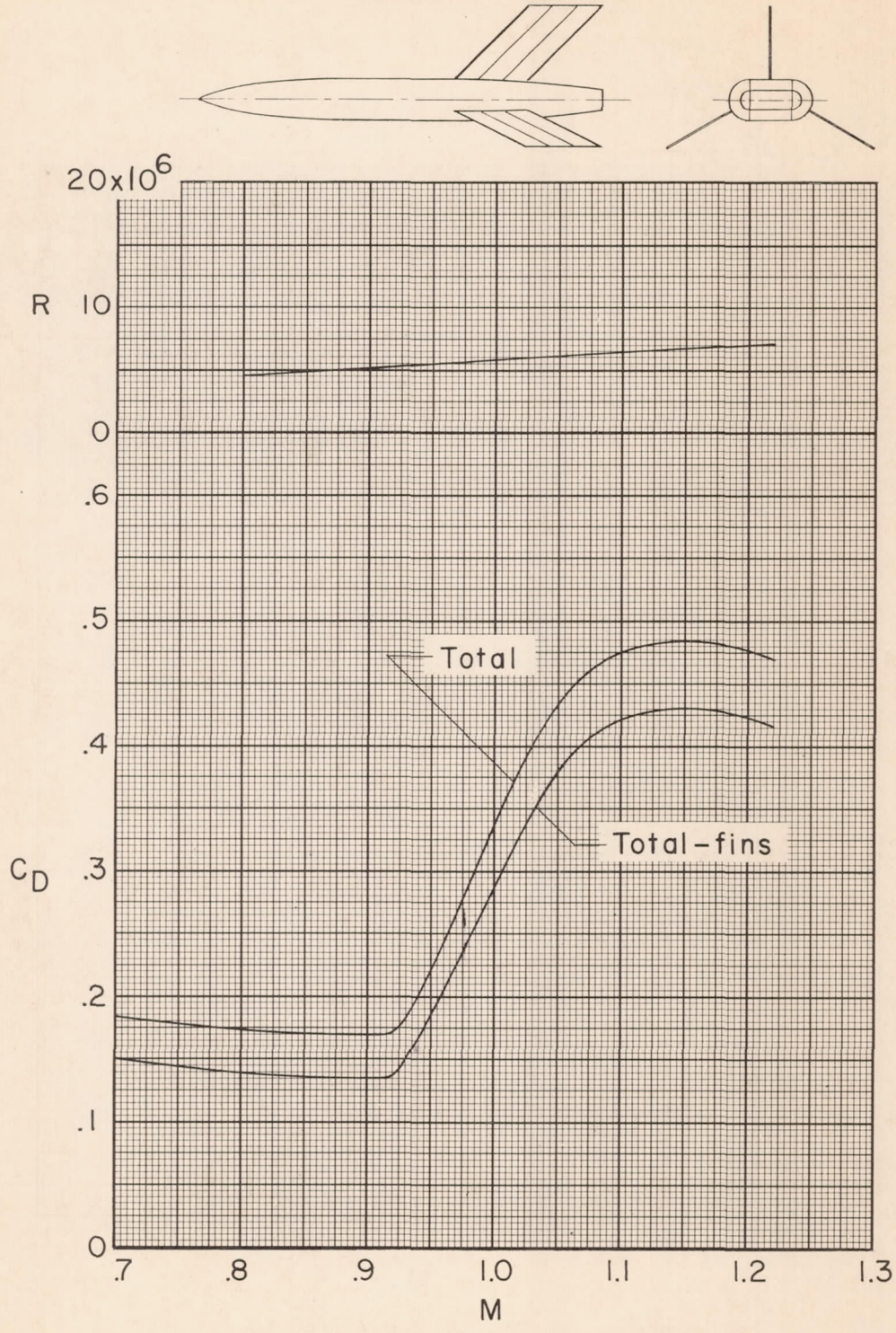
(p) F-94 tank (l/d = 7.15).

Figure 5.- Continued.



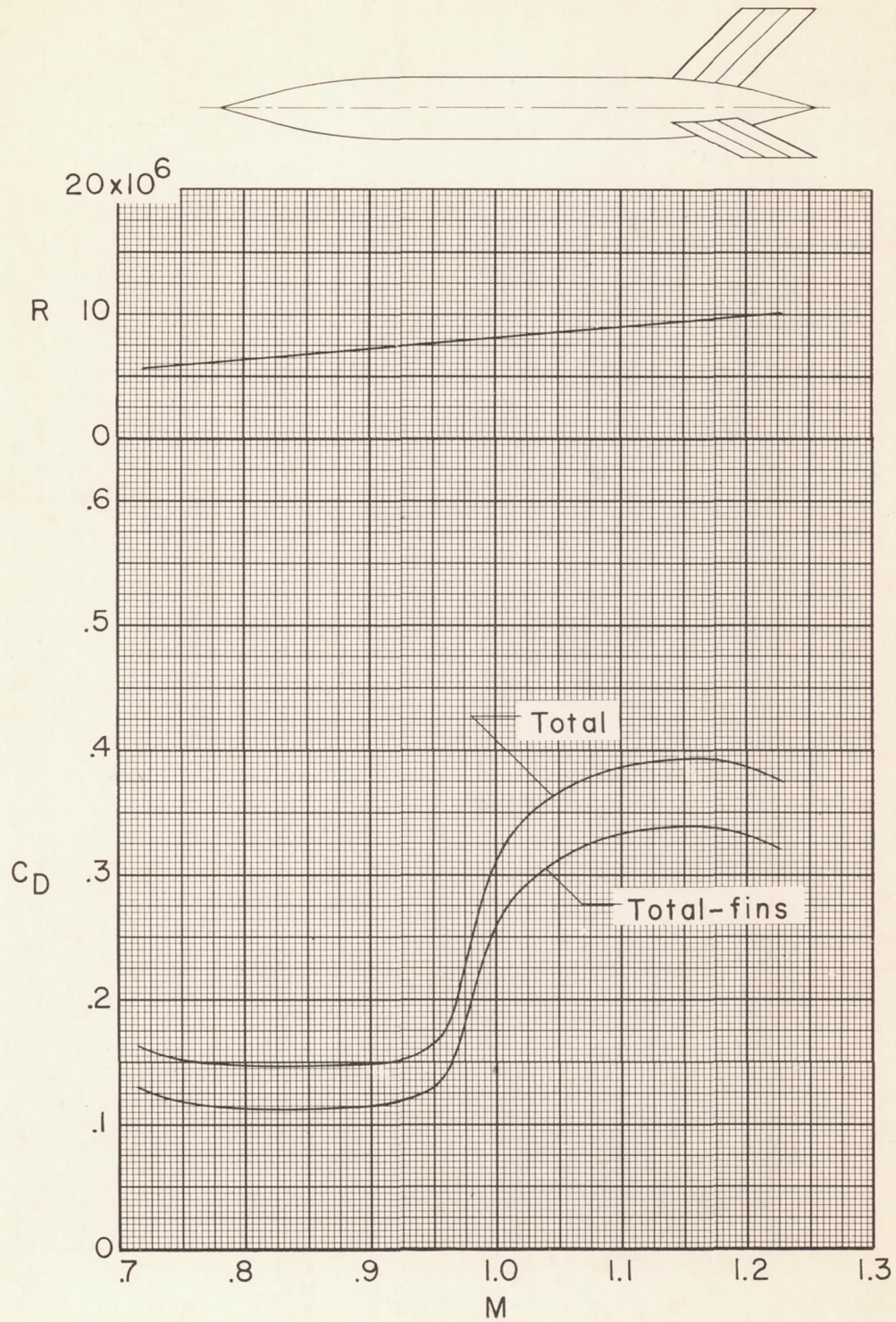
(q) Nacelle model 1 (l/d = 11.08).

Figure 5.- Continued.



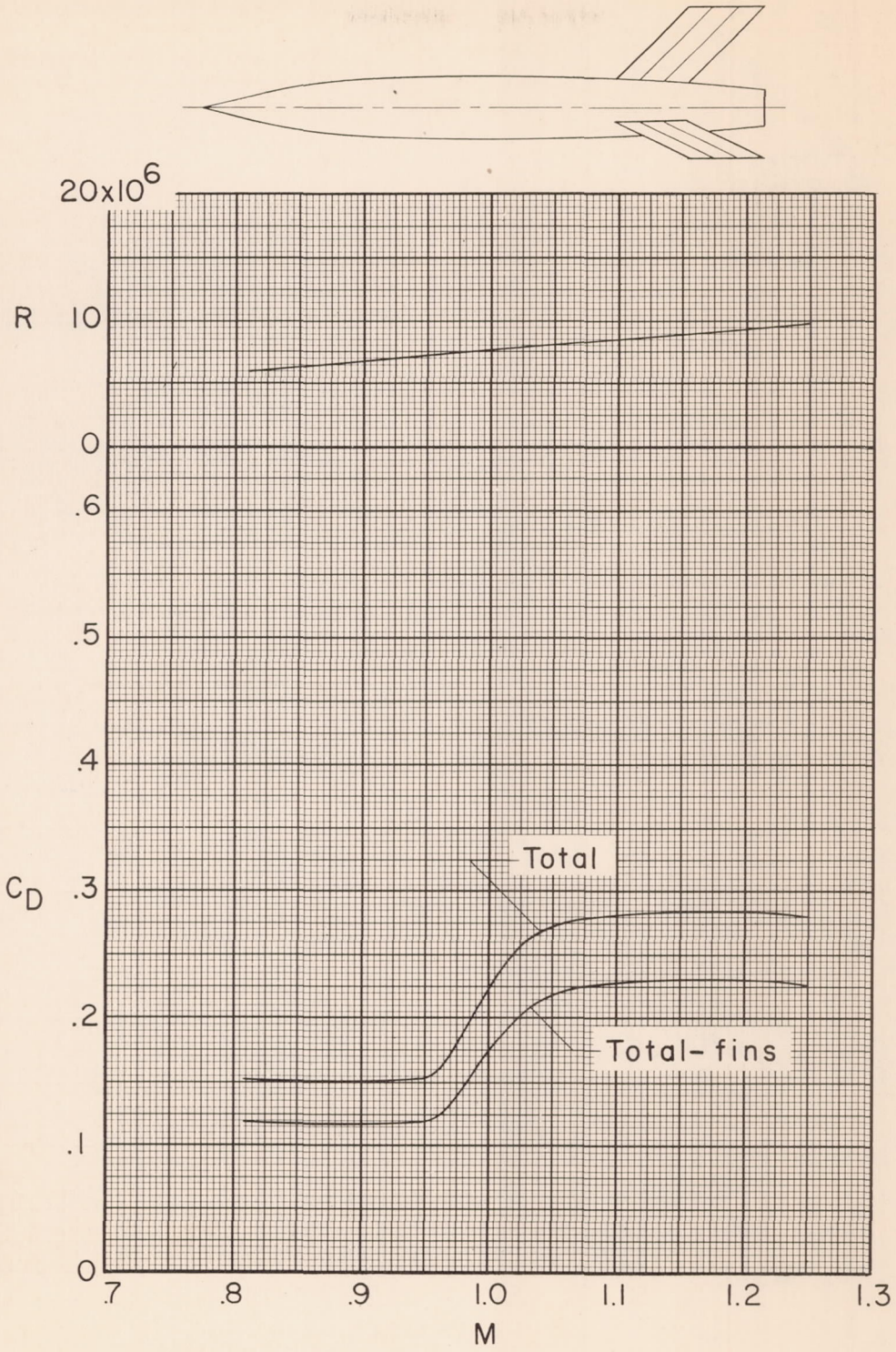
(r) Nacelle model 2 (l/d = 6.40).

Figure 5.- Continued.



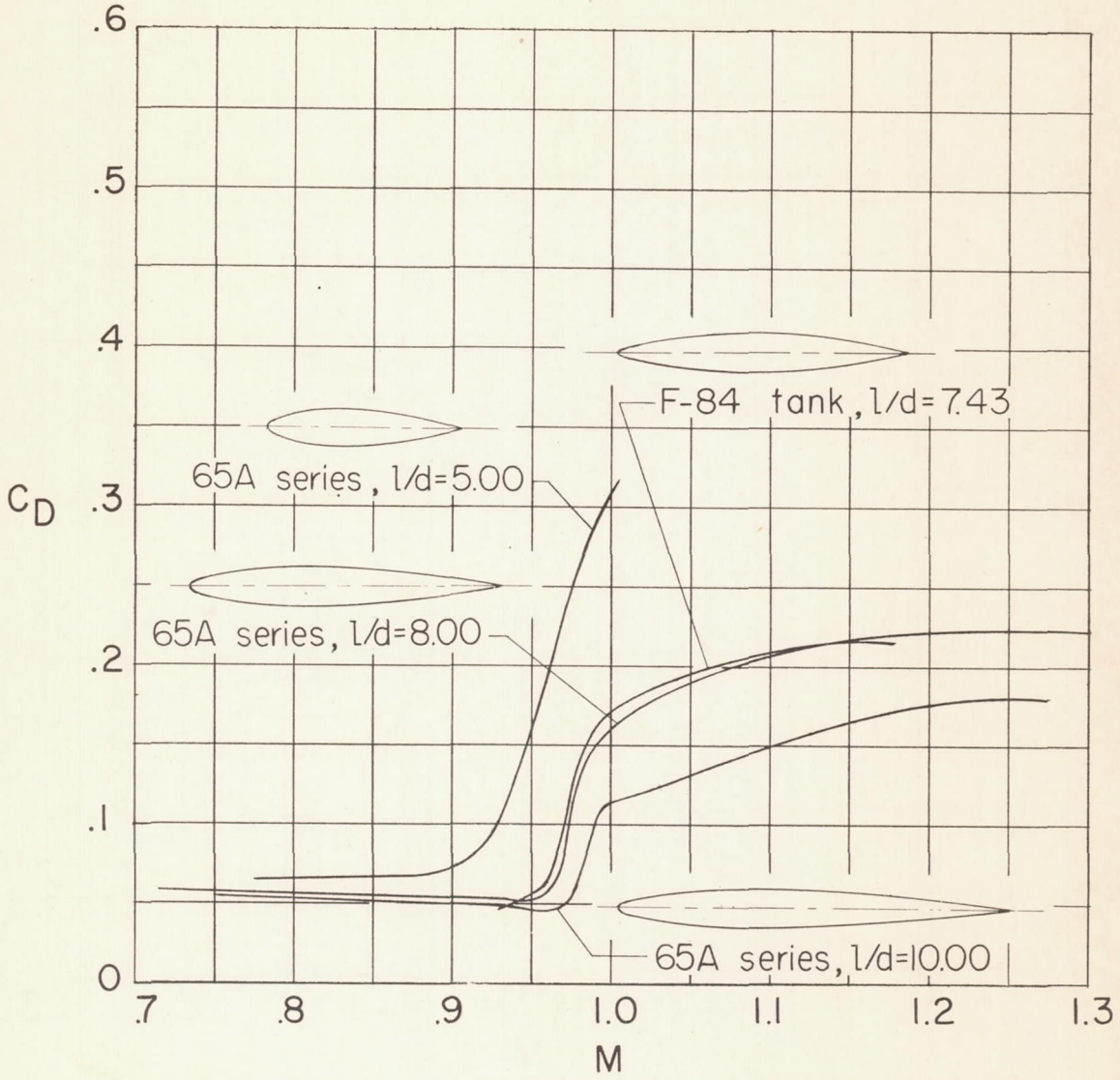
(s) Nacelle model 3 (l/d = 9.51).

Figure 5.- Continued.



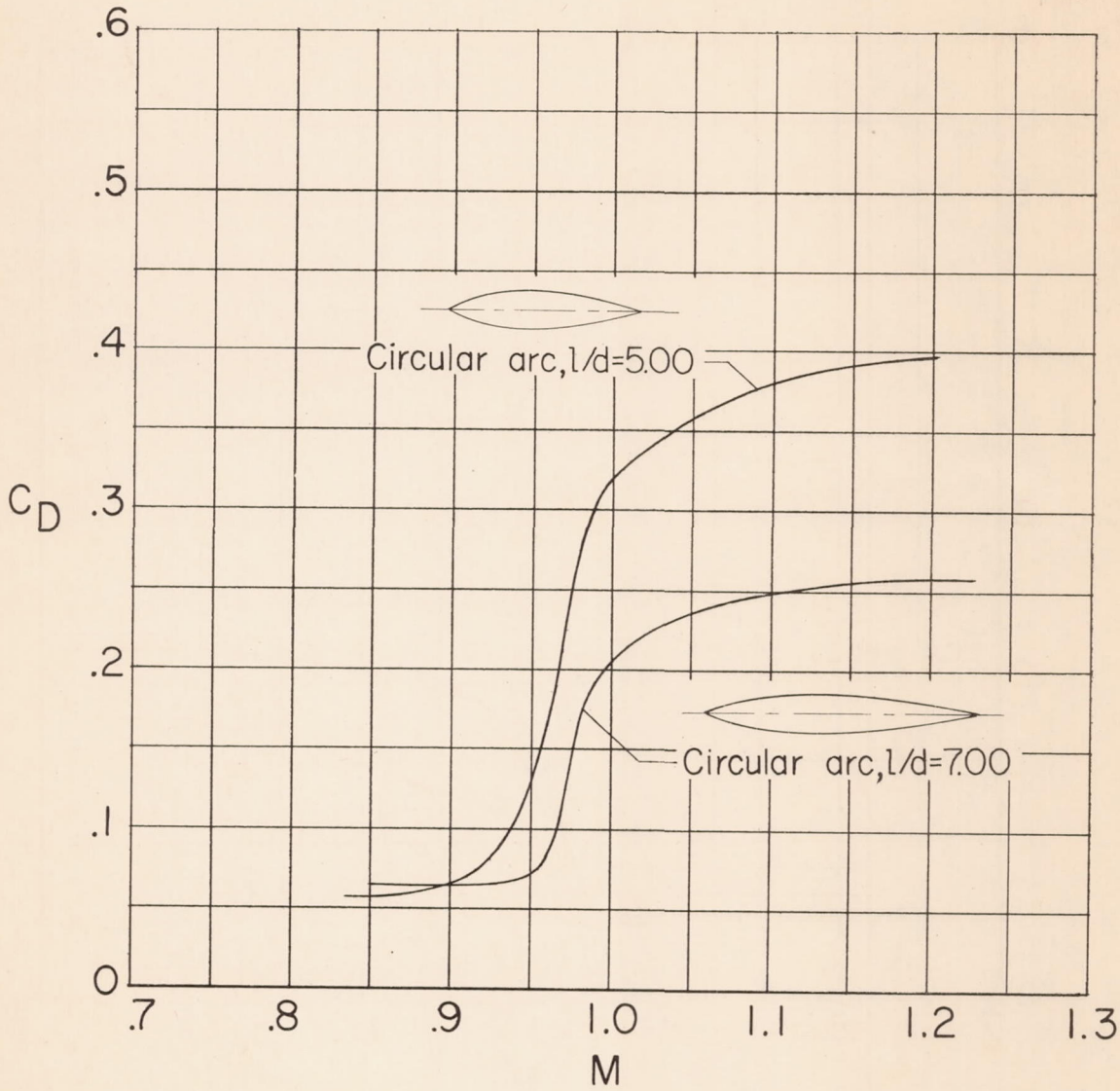
(t) Nacelle model 4 (l/d = 8.81).

Figure 5.- Concluded.



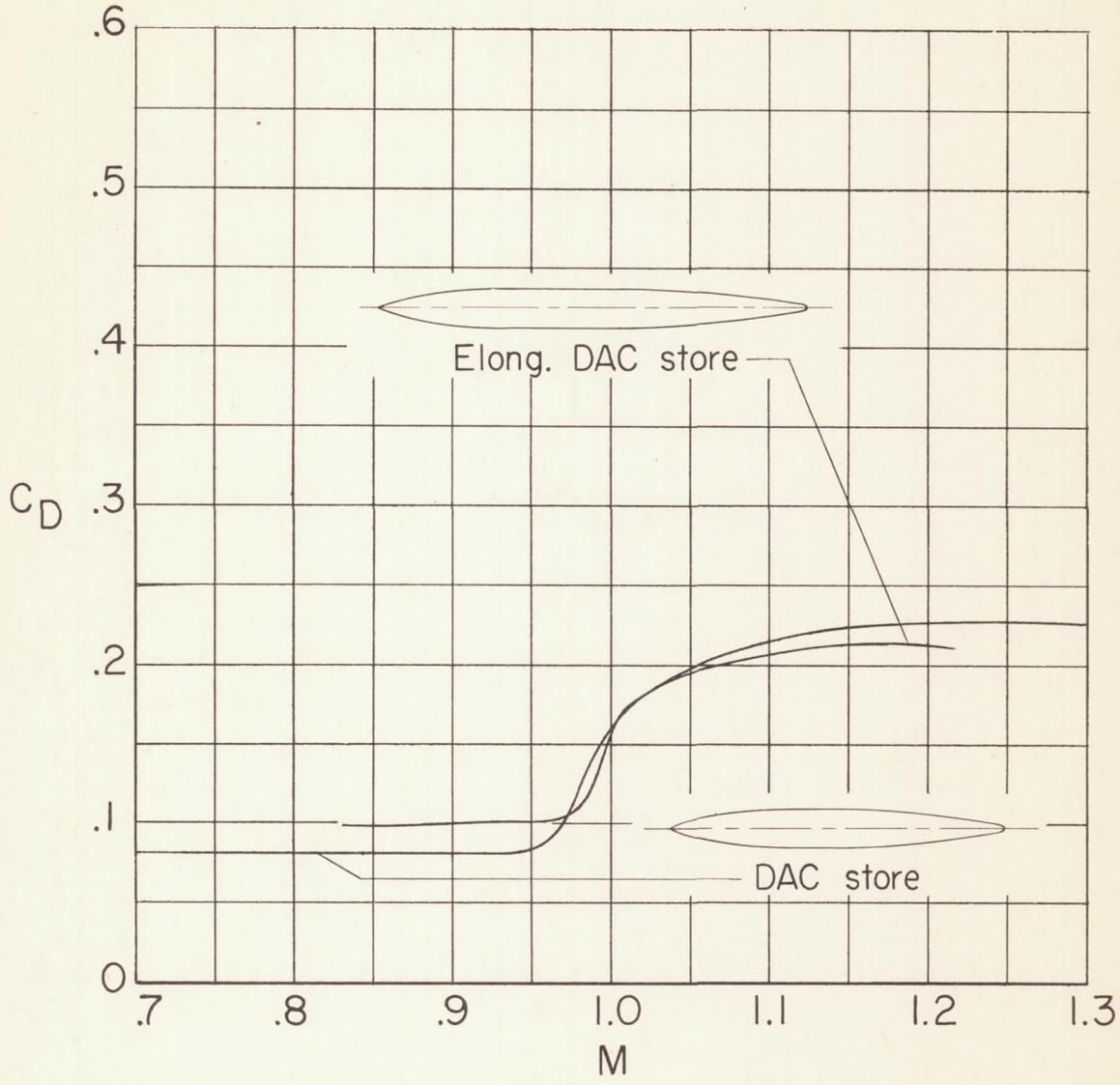
(a) NACA 65A-series bodies and F-84 tank.

Figure 6.- Fineness-ratio effects.



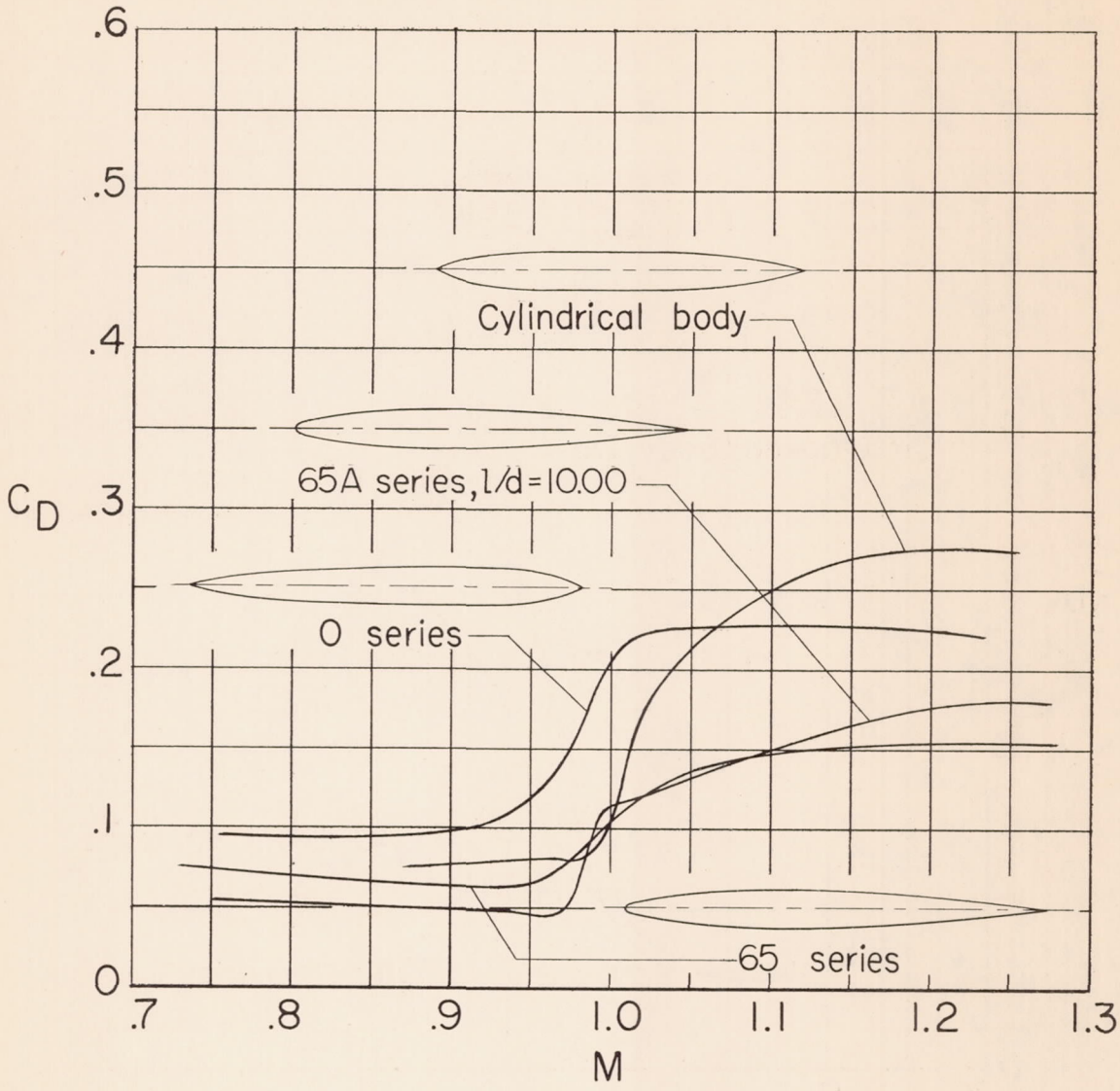
(b) Circular-arc bodies.

Figure 6.- Continued.



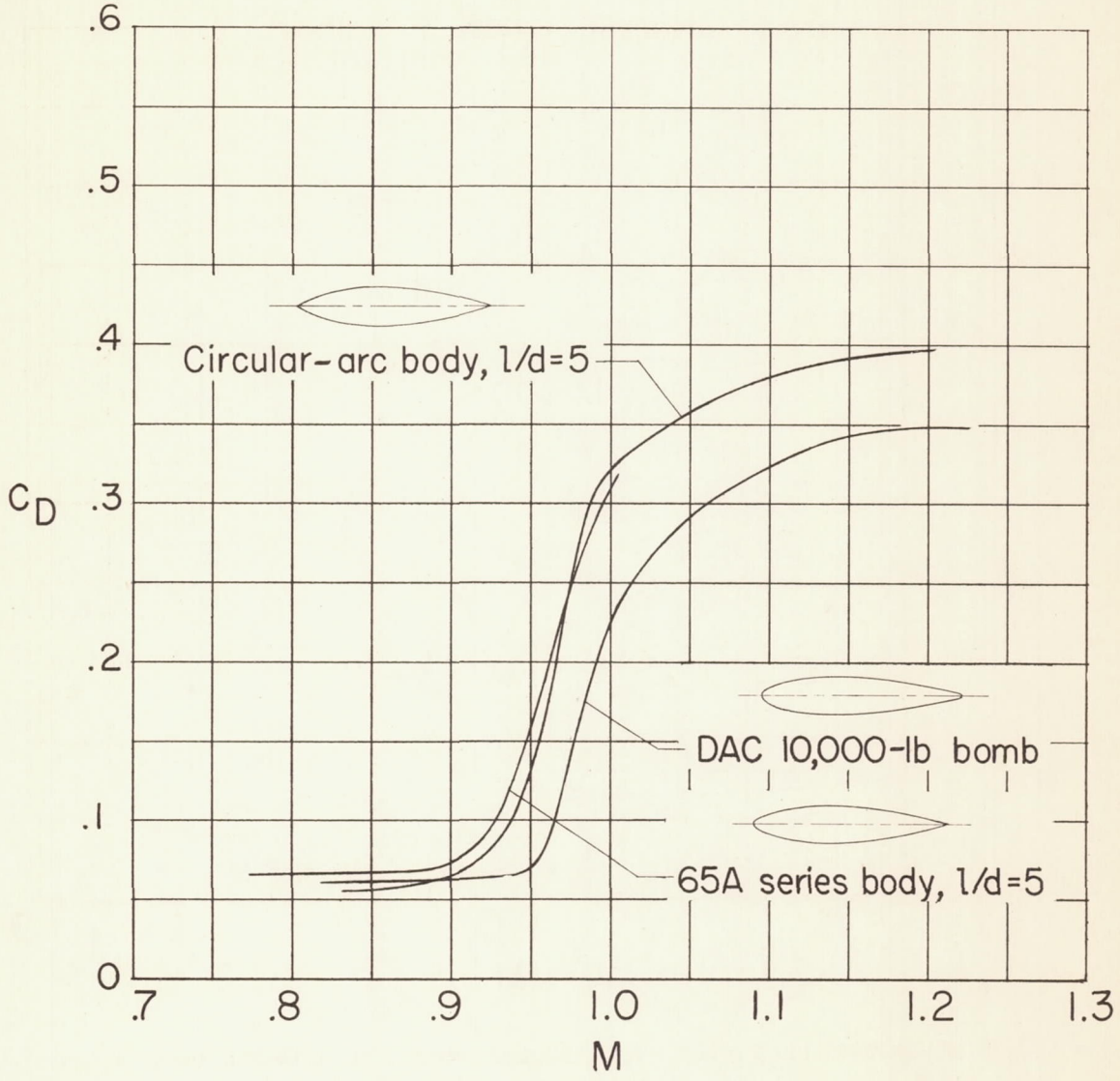
(c) DAC store and elongated DAC store.

Figure 6.- Concluded.



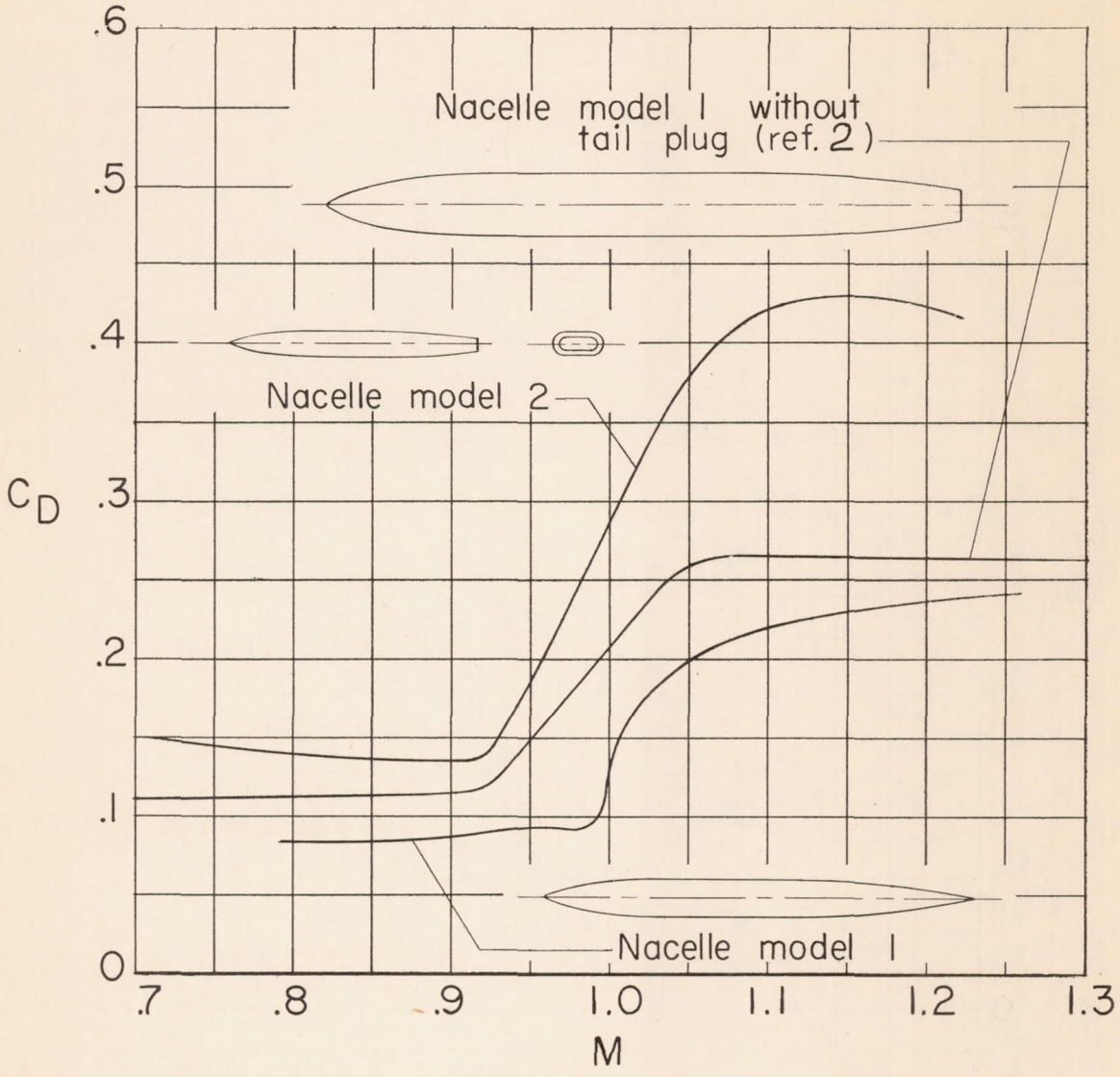
(a) NACA 65-series body, NACA 65A-series body, NACA 0-series body, and cylindrical body.

Figure 7.- Shape effects.



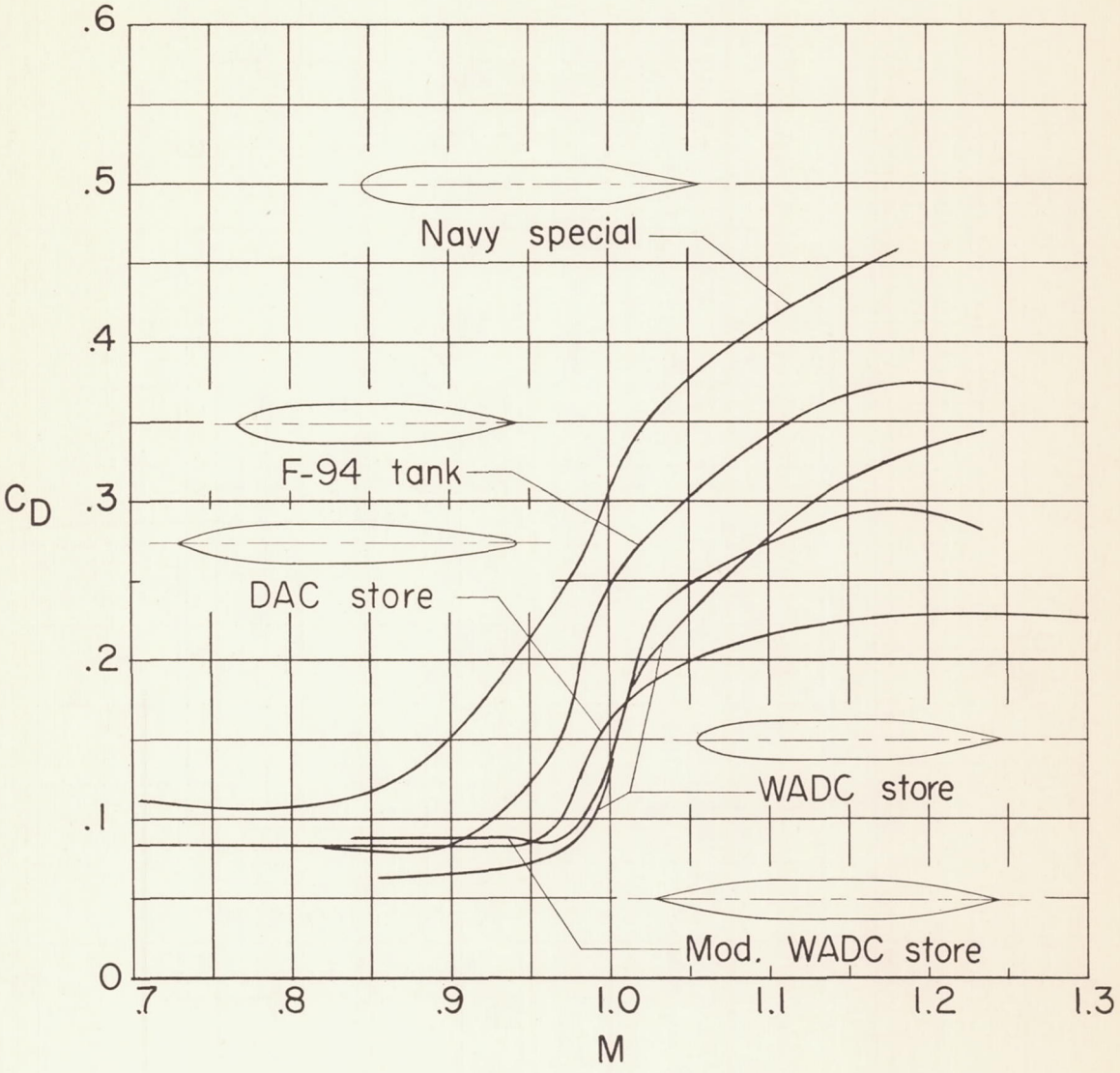
(b) NACA 65A-series body, circular-arc body, and DAC 10,000-lb bomb.

Figure 7.- Continued.



(c) Nacelle models 1 and 2 and nacelle model 1 without tail plug.

Figure 7.- Continued.



(d) WADC store, modified WADC store, DAC store, Navy special 1A-2000 lb store, and F-94 tank.

Figure 7.- Concluded.

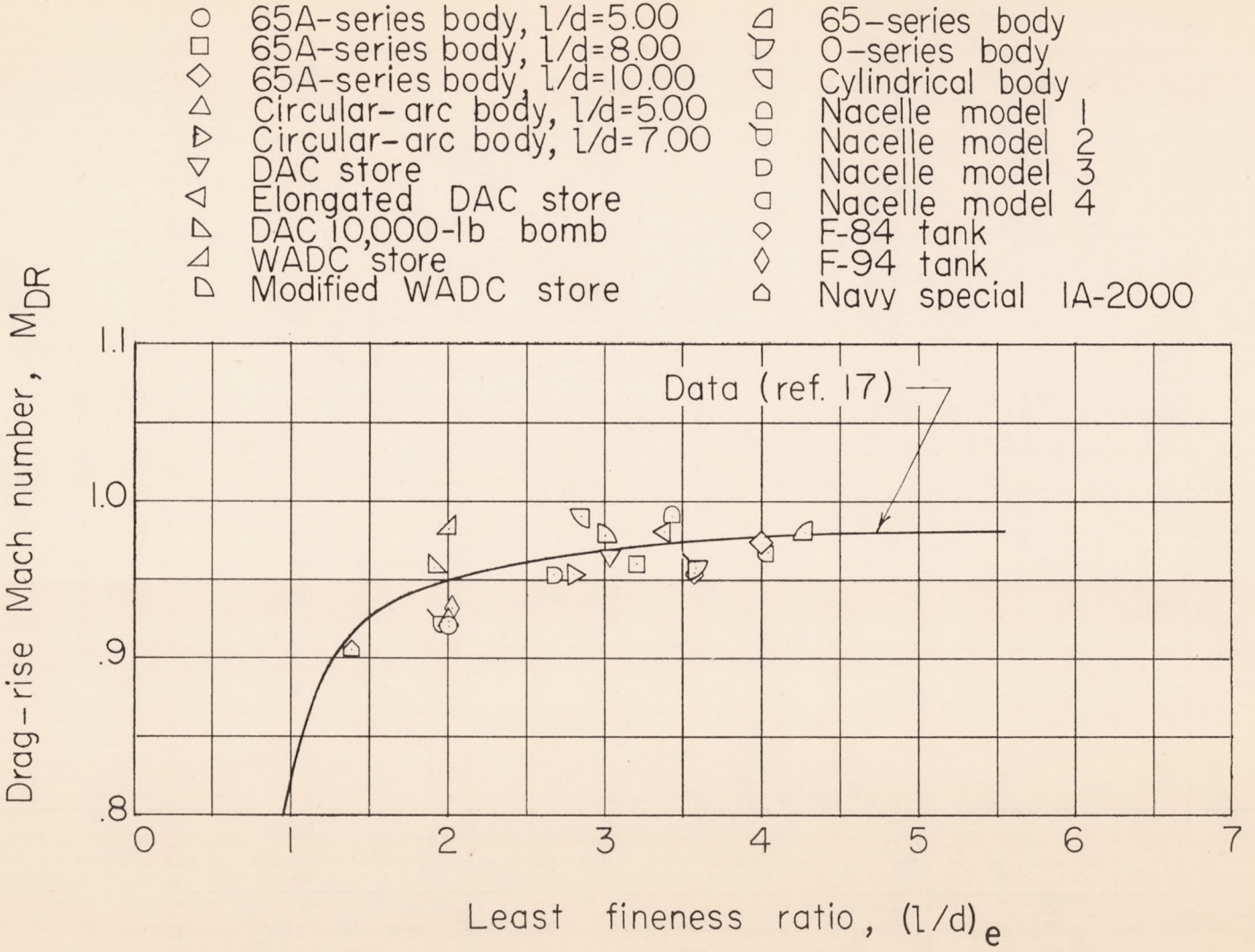


Figure 8.- Drag-rise Mach number as a function of the fineness ratio of the shorter extremity. Flagged symbols indicate afterbody.

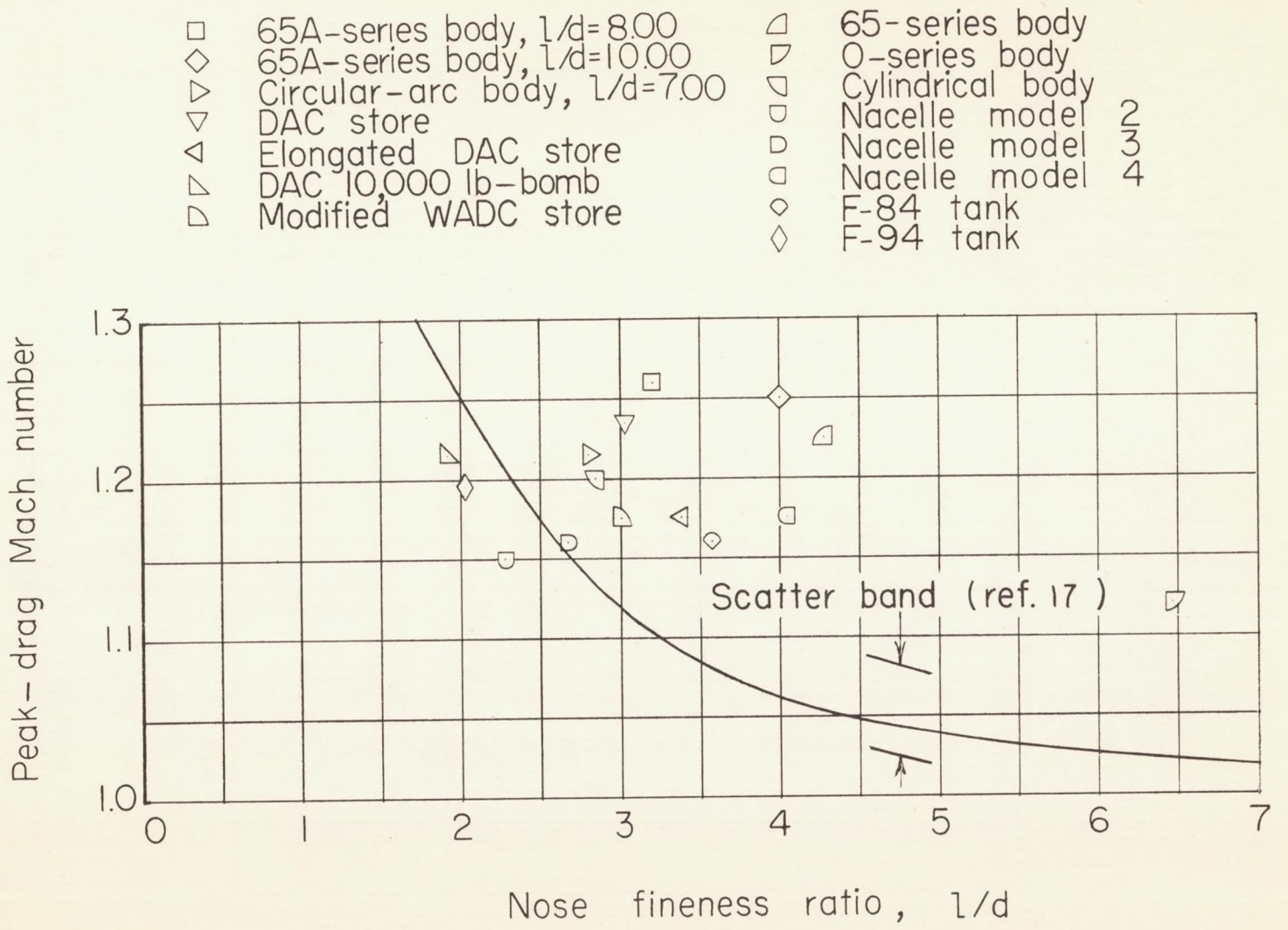


Figure 9.- Mach number at which peak drag occurs as a function of nose fineness ratio.

CONFIDENTIAL

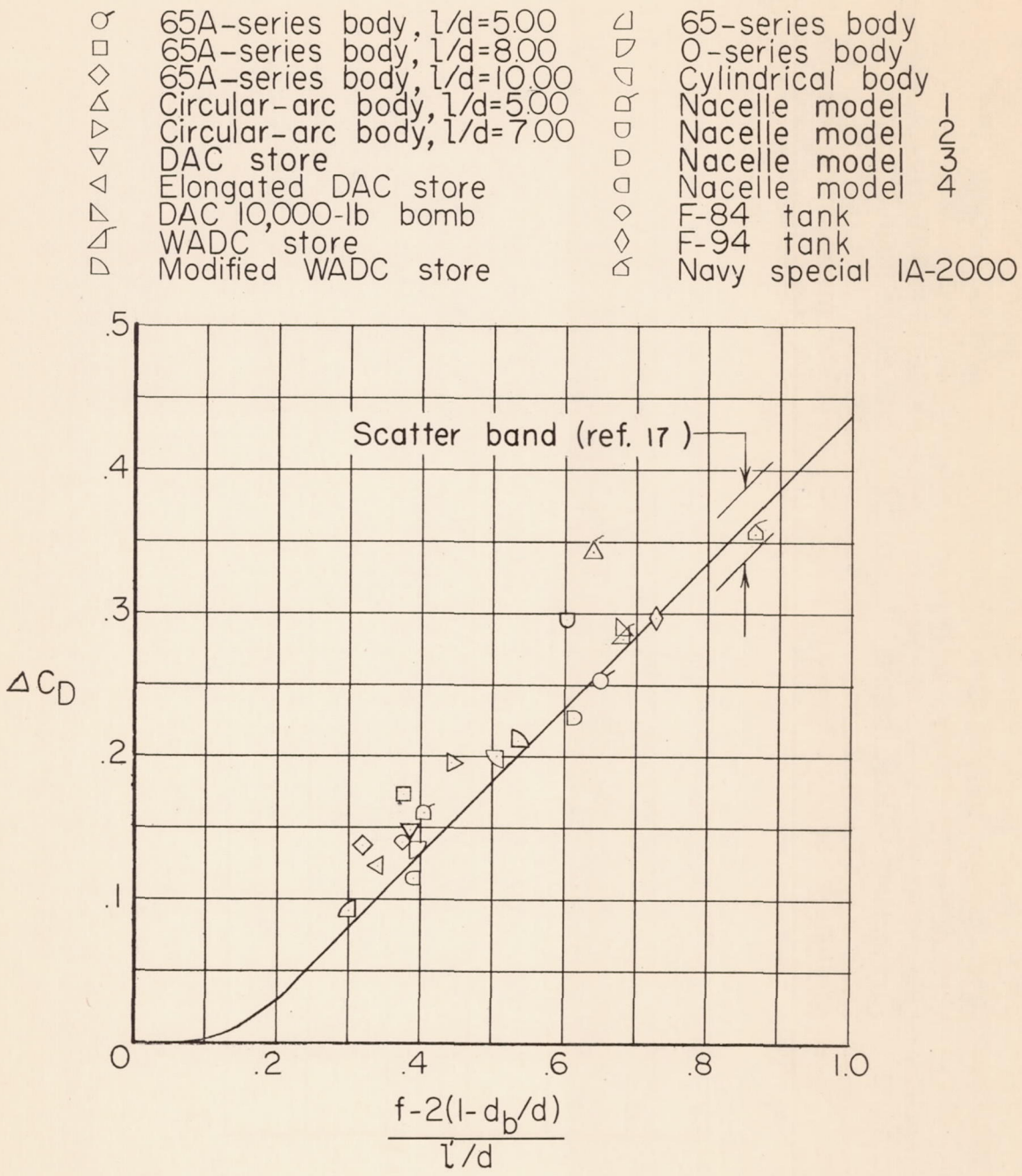


Figure 10.- Peak-pressure drag as a function of the correlation factor of reference 17. Flagged symbols indicate C_D still increasing at maximum test Mach number.

NACA-Langley - 3-11-55 - 350

~~CONFIDENTIAL~~

CLASSIFICATION CHANGED TO:
Unclassified
Per Abstract 121
11-4-57

~~CONFIDENTIAL~~